

**Nevada Water Resources Research Institute  
Annual Technical Report  
FY 2014**

# Introduction

Success and dedication to quality research has established the Division of Hydrologic Sciences as the recognized "Institute" under the Water Resources Research Act of 1984 (as amended). A total of 54 Institutes are located at colleges and universities in the 50 states, the District of Columbia, Puerto Rico, and the U.S. Virgin Islands.

The primary mission of the Nevada Water Resources Research Institute is to inform the scientists of Nevada.

## Research Program Introduction

Nevada is the most arid state in the United States and it is experiencing significant population growth and possible future climate change. With competing water demands for agricultural, domestic, industrial, and environmental uses, issues surrounding water supply and quality are becoming more complex, which increases the need to develop and disseminate sound science to support informed decision making.

As the NWRRI, the continuing goals of DHS are to develop the water sciences knowledge and expertise that support Nevada's water needs, encourage our nation to manage water more responsibly, and train students to become productive professionals. Therefore, DHS has chosen to make a valuable contribution to water research and education in Nevada by judiciously distributing its Section 104 research funds among numerous subject areas. Projects must be of significant scientific merit (as determined by the review process) and relevant to Nevada's total water program to be considered worthy of funding.

To ensure collaboration and coordination among water-related entities throughout the state, DHS maintains a Statewide Advisory Council on Water Resources Research composed of leading water officials who may be called upon to assist in selecting the research projects that will be supported by Section 104 funds.

# Optimization of ozone-biological activated carbon treatment for potable reuse applications

## Basic Information

<b>Title:</b>	Optimization of ozone-biological activated carbon treatment for potable reuse applications
<b>Project Number:</b>	2013NV194B
<b>Start Date:</b>	3/1/2013
<b>End Date:</b>	6/30/2015
<b>Funding Source:</b>	104B
<b>Congressional District:</b>	NV003
<b>Research Category:</b>	Water Quality
<b>Focus Category:</b>	Water Quality, Treatment, Water Supply
<b>Descriptors:</b>	None
<b>Principal Investigators:</b>	Daniel Gerrity

## Publications

1. Selvy, A., D. Gerrity. 2014. Optimization of Ozone-Biological Activated Carbon Treatment for Potable Reuse Applications. Nevada Water Resources Association 2014 Annual Conference, Las Vegas, NV, Jan. 2014.
2. Selvy, A., D. Gerrity. 2015. Impacts Of Ozone Dose And Empty Bed Contact Time On Total Organic Carbon Removal Through Ozone-Biological Activated Carbon Treatment. 19th Annual Water Reuse and Desalination Research Conference, Huntington Beach, CA, May 2015.

# Final Report

## 1.0 Problem and Research Objectives

In the face of climate change, pollution, and population growth, water scarcity has become a global threat. Many populations have witnessed their drinking water sources dwindle to an unsustainable level. These severe conditions have sparked interest in potable reuse as an increasingly viable alternative to typical ‘pristine’ drinking water sources. Although potable reuse has been practiced for decades, the public has become more supportive of the concept over the past few years based on the historical success of several benchmark facilities in the United States and abroad (Gerrity et al., 2013). Many municipalities are considering implementing their own projects, but there is considerable debate as to the level of treatment needed to ensure protection of public health.

Among existing potable reuse guidelines and regulations, the California Division of Drinking Water (DDW) provides the most stringent requirements for water quality (CDPH, 2014). Currently, the best way to meet these standards is through the use of full advanced treatment (FAT), which consists of reverse osmosis (RO) and an advanced oxidation process (AOP). Although extremely effective, RO is energy intensive and produces a concentrated brine solution that is both difficult to dispose of and an ecological concern in coastal regions (Gerrity et al., 2014). Alternative treatment trains composed of ozone and biofiltration, particularly biological activated carbon (BAC), have been employed in several locations throughout the world, but these systems have not yet been optimized and are unable to compete with RO-based treatment trains on the basis of total organic carbon (TOC) removal and reductions in total dissolved solids (TDS). While RO-based treatment trains have been known to remove TOC to the  $\mu\text{g/L}$  level, ozone-BAC trains have yet to achieve this threshold.

With the exception of TOC and TDS, which are generally more relevant to aesthetics rather than public health, ozone-BAC is capable of producing a water quality similar to that of RO-based treatment trains on the basis of pathogen reduction, trace organic contaminant mitigation, and a variety of other parameters. There are also significant energy and cost savings for the ozone-BAC alternative so there is an incentive to optimize such treatment trains to achieve greater TOC removal. This process requires up to 70% less in capital costs and 80% less in operation and maintenance (O&M) costs in comparison to FAT (Gerrity et al., 2014).

The objective of this study was to identify the necessary operational conditions needed for ozone-biofiltration treatment trains to compete with FAT on the basis of TOC reduction. The original hypothesis was that by coupling greater effluent organic matter transformation via increased ozone doses with longer empty bed contact times, ozone-biofiltration systems could achieve better TOC removal and possibly approach the 0.5-mg/L threshold for TOC set by the California DDW.

## 2.0 Methodology

### 2.1 Pilot-Scale Reactor

#### 2.1.1 Construction and Operation

A 0.6 liter-per-minute (lpm) pilot-scale reactor was constructed at a water recycling facility in the Las Vegas metropolitan area. It consisted of 12 ozone contactors and six biofilters, which were used to treat full-scale membrane bioreactor (MBR) filtrate. The flow rate through the system was measured with an in-line flow meter. The addition of sodium chloride for a tracer study, which was used to determine the hydraulic retention time of the ozone contactor, was achieved through a sample injection port followed by a static mixer. Ambient air, oxygen, or ozone was introduced through a Venturi injector downstream of the static mixer. Concentrated oxygen was achieved with a portable medical system equipped with molecular sieves (AirSep, Denver, CO). The oxygen was generated at a flow rate of between 0.5 and 2 lpm and a pressure of 20 psig throughout the study. After passing through an air filter to remove particulates, the oxygen traveled to a Magnum-600 air dryer (Ozone Solutions Inc., Hull, Iowa) to remove any moisture from the oxygen prior to reaching the Nano dielectric ozone generator (Absolute Ozone, Edmonton, AB, Canada). The output from the ozone generator traveled either through a bypass line to a catalytic destruct unit or to the Venturi injector, where the ozone was injected into the process flow. The bypass line was controlled by a standard gas flow meter. In addition to check valves, the feed gas line was equipped with a water trap that prevented water from entering the feed gas tubing and backing up into the generator, as well as a pressure gauge to monitor feed gas pressure entering the Venturi injector.

The ozonated water then traveled to the 12 ozone contactors connected in series (four were one inch in diameter and eight were two inches in diameter); samples were collected from sample ports located at the bottom of the contactors. Ozone off-gas was collected in Teflon tubing at the top of each contactor and was sent to a catalytic destruct unit. The ozone off-gas line was also protected by a water trap that prevented water from reaching the catalytic destruct unit. Ozone doses were estimated by measuring differential UV<sub>254</sub> absorbance after ozonation and then estimating the ozone to total organic carbon (O<sub>3</sub>/TOC) ratio based on established correlations in the literature (Gerrity et al., 2012) and an independent site-specific correlation (*Section 4.3.1*).

The effluent from the final ozone contactor fed five parallel, 1-inch diameter biofilter columns. At various times throughout the project, these biofilter columns were filled with either 1.2-mm diameter anthracite provided by the San Jose Creek Water Reclamation Plant, 0.95-mm diameter exhausted GAC (Norit 820, Cabot Corporation, Alpharetta, GA) from the F. Wayne Hill Water Resources Center (Gwinnett County, GA), or a proprietary denitrifying biocatalyst (hereafter referred to as "BC"). The column-to-media diameter ratios were approximately 21:1 and 27:1 for the 1.2-mm BAC and 0.95-mm BAC, respectively. The BC was manufactured as a porous polyvinyl alcohol (PVA) bead containing denitrifying microorganisms. The BC has historically

been used in suspended growth (i.e., activated sludge) systems so this was the first evaluation of the BC in a packed-bed configuration. A separate control biofilter (containing 1.2-mm anthracite) received non-ozonated pilot influent (i.e., MBR filtrate) to allow for the evaluation of organic matter removal with and without the synergistic effects of ozonation. An experimental anthracite column, the biocatalyst column, and the control anthracite column were all operated at the same EBCT during long-term operation to allow for direct comparisons of treatment efficacy. Biofilter sample ports for treated water were located at the bottom of each column, and the flow rates (and EBCTs) were controlled by independent needle valves. Samples of biofilter media were also collected periodically from dedicated sample ports to evaluate the development of the microbial community. The microbial community in the biofilters will be discussed in *Section 4.4*.

Figure 1 illustrates the layout of the pilot-scale reactor, and corresponding photos of the ozone contactors and biofilter columns are provided in Figures 2A and 2B, respectively. In Figure 1, the pink asterisks mark the sampling locations for treated water from the biofilters, the white “X’s” represent the lower media sampling locations at a 17.5-inch filter media depth, and the blue “X’s” signify the upper media sampling locations at a depth of 5.5 inches. The green circles denote the non-filtered water samples. The influent sample port was located prior to ozone injection into the water stream, and the effluent sample location was located after the ozone contactors. The effluent samples consisted only of ozonated water. The BC column did not have any media sample locations; the samples had to be collected by backfilling the column with water and expanding the media to the top where it could be collected.

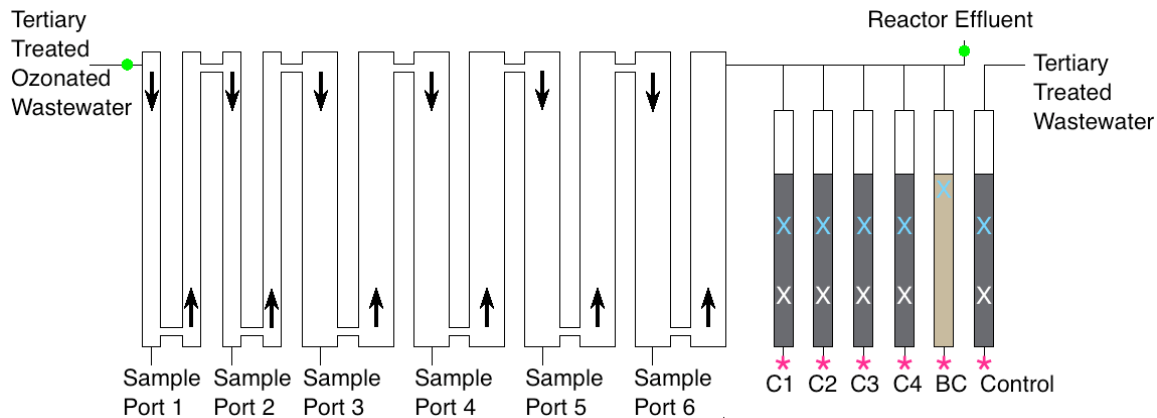


**Figure 1. Schematic of pilot-scale reactor.**

During the initial long-term operation of the pilot, C1-C4 and the Control were filled with 1.2-mm diameter anthracite. During later phases of the project, C3 was switched to the 0.95-mm diameter exhausted GAC (i.e., BAC). The column containing the biocatalyst is denoted as BC.

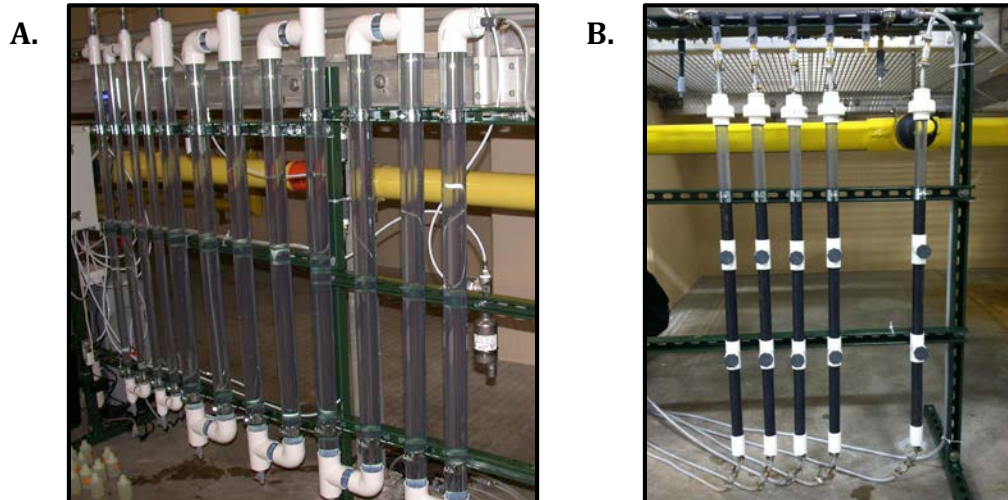


Figure 2. Photos of the (A) ozone contactors and (B) biofilters.

### 2.1.2 Backwashing

Backwashing of the pilot-scale biofilter columns was performed based on performance observations. When accumulation in the filters was too high, the flow rate would drop significantly. This was used as an indication of the need for backwashing. This method was chosen (as opposed to regular time intervals) because of the variability of the influent water quality and flow rate, which would impact the filter run time.

The biofilter effluent tubing was detachable making it possible for the backwash tubing to be attached at the bottom of the filter. The top of the filter was also detachable. Membrane bioreactor effluent was used as the backwash water and was pumped through the bottom of the filters using a MasterFlex peristaltic pump (Cole Palmer, USA). Backwashing flow rates varied between each filter and over time. A bed expansion of 34% was targeted and the flow rate adjusted accordingly. A 34% bed expansion was chosen because it was within typical values found in literature. Backwash duration was ten minutes. No air scour or chlorination was used.

### 2.1.3 Start-up

Initially, five columns were filled with the 1.2-mm anthracite and fed membrane bioreactor effluent without ozonation (C1, C2, C3, C4, and control). The total organic carbon was monitored for indications of microbial growth. Initially, the goal was to develop the microbial community without the use of ozone. This would allow for the identification of a TOC removal baseline from which the synergistic impacts of ozone could be quantified. However, limited TOC removal and biological growth (based on the adenosine triphosphate (ATP) measurements described later) were observed during long-term operation of the pilot prior to start-up of the ozone generator.

Initially, it was hypothesized that there was an insufficient seeding of bacteria because of the membrane component of the MBR, which is essentially an impermeable barrier to larger microorganisms. To supplement the bacteria already attached to the media prior to start-up, the columns were seeded with secondary treated wastewater effluent from a separate full-scale facility for 24 hours each. After observing minimal improvements in system performance, it was then hypothesized that the MBR filtrate may have been overly recalcitrant, thereby limiting the supply of a suitable carbon source for any attached bacteria. Potential solutions included seeding the reactors with an alternative carbon source, such as acetate or methanol, or implementing ozonation to transform the recalcitrant effluent organic matter (EfOM) into a more bioavailable supply. Continuous ozonation was identified as the preferred alternative. Four months after start-up, the ozone system was initiated to enhance biological growth in the filters.

A proprietary biocatalyst containing denitrifying bacteria was provided as an alternative biofilter media for this study. It is made of a porous material, which allows for the passage of water and dissolved constituents and subsequent interaction with the bacteria. The BC was installed two months after ozone start-up but did not receive ozonated water until three months after installation. During this time, the control biofilter was receiving ozonated effluent to promote biological growth. After the biological community stabilized in the control column, the control and BC column positions were switched so that the control and BC were receiving non-ozonated and ozonated effluent, respectively. The empty bed contact times were then adjusted and maintained at C1 (ozone+anthracite) = 5, C2 (ozone+anthracite) = 10, C3 (ozone+anthracite) = 10, C4 (ozone+anthracite) = 15, Control (anthracite only) = 10, and BC (ozone+biocatalyst) = 10 minutes for a three-month period. During this time, the impact of EBCT on TOC removal was monitored.

During testing, several issues were observed with the BC, all of which were related to using the material in a configuration for which it was not designed. For example, the BC beads would not fluidize during backwashing. This could be attributed to the low density of the BC beads and/or its material properties coupled with the peristaltic pump used for backwashing. A flow rate of approximately 56 mL/min (the lowest setting on the pump) resulted in full bed expansion, but there was insufficient agitation for fluidization to take place because the BC consisted of a soft material that would cause the beads to stick together and form a thick cake. For this reason, the BC column was never effectively backwashed throughout the study. Also, the BC beads began to compact after about five months of operation, which drastically inhibited flow through the column. It was difficult, and sometimes impossible, to achieve the desired flow rates through the BC column. After initial signs of compaction, the BC column was backfilled with water, which allowed time for the beads to expand to their original form. However, the beads would slowly compact once filtration was resumed, and after several cycles, the beads began to compact instantly. Again, the BC is typically used in suspended growth systems where compaction is not a concern. Finally, the true purpose of the BC is denitrification, which generally requires anoxic conditions (i.e., nitrite/nitrate serve as the electron acceptor in the absence of dissolved oxygen). Ozonation leads to supersaturation of treated water with dissolved oxygen, which inhibits the

denitrification process. As will be described later, the BC initially performed well for the removal of bulk organic matter, presumably due to the growth of bacteria on the outside of the beads, but modified process configurations would be necessary for future BC implementation.

Seven months after ozone initiation, the media in C3 was replaced with exhausted 0.95-mm Norit 820 GAC. This was done to provide a direct comparison between anthracite and exhausted GAC as potential surfaces for biofilm development. Due to the pore structure and high specific surface area of virgin GAC, it is often used as an adsorbent material for the removal of trace organics, bulk organic matter, and other water contaminants. GAC eventually loses its adsorptive capacity, which results in contaminant breakthrough and ultimately exhaustion. If adsorption is required to achieve specified operational criteria, the GAC is then replaced or regenerated, which increases operational costs. In a biofiltration application, the adsorptive capacity is less important because the intent of the media is to serve as a surface for biofilm attachment and growth. Although the pores are generally too small for bacteria to penetrate, the exhausted GAC, or BAC, still has a relatively high specific surface area, which is advantageous for development of the microbial community.

After examining the impact of EBCT on reactor performance, all columns were maintained at an EBCT of ten minutes in preparation of the kinetics tests discussed in *Section 2.2*.

## **2.2 Methodology for Performing Kinetics Tests**

Three kinetics tests were performed, each at a different ozone dose. The ozone dose was held constant while the EBCTs of the filters were adjusted in small intervals. After adjustments to the EBCTs were made, a time equivalent to three hydraulic retention times was allowed prior to sampling. This was done to allow sufficient time for stabilization. The range of hydraulic loading rates employed during the kinetics tests was 0.51 – 119 cm/min (0.12 – 29 gpm/ft<sup>2</sup>).

The first kinetics test was performed at a mass-based ozone to total organic carbon ratio ( $O_3/TOC$ ) of 0.35. The EBCTs were increased step-wise from 1.75 minutes to 10 minutes. Ten sample events were performed during this test. The second kinetics test utilized an  $O_3/TOC$  ratio of 1.12. The EBCTs were varied between 2-30 minutes; the order of the EBCTs was random to determine if any systematic error occurs from increasing the EBCT step-wise. For the third test, an  $O_3/TOC$  of 0.62 was applied. Again, 10 sampling events were performed at EBCTs between 2 and 14 minutes.

## **2.3 Methodology for Ozone Demand Decay Testing**

An ozone demand decay study was performed on the source water using the indigo trisulfonate colorimetric method for dissolved ozone. Potassium indigo trisulfonate is dark blue in color but will quickly decolorize in the presence of ozone as the chemical is oxidized. A spectrophotometer is used to determine the absorbance of the indigo trisulfonate solution at 600

nm, which is directly related to the strength of the blue color. The extent of decolorization, or bleaching, during ozonation is directly correlated with the dissolved ozone concentration.

For this study, an ozone demand decay test was performed in a batch configuration. Five gallons of source water were collected and ozonated at the following O<sub>3</sub>/TOC ratios: 0.25, 0.5, 1.0, and 1.5. Then, 10 mL of potassium indigo trisulfonate test solution were added to several 100 mL volumetric flasks that had been previously weighed. The ozonated source water was added to a single flask at specified time steps (every 30 seconds for the first two minutes, every minute for the next eight minutes, and then every two minutes thereafter). A sufficient sample volume was added to each flask to induce a noticeable color change due to the combined effects of oxidation and/or dilution. The flasks, which now contained indigo trisulfonate plus sample, were weighed to determine the mass of sample added, which was later converted to volume. The absorbance of each sample was then measured with a spectrophotometer, and the absorbance of each sample was converted to a dissolved ozone concentration using Eq. 1:

$$O_3(\text{mg/L}) = \frac{V_{\text{blank+indigo}} \times \text{Absorbance}_{\text{blank}} - V_{\text{sample+indigo}} \times \text{Absorbance}_{\text{sample}}}{f \times V_{\text{sample}} \times b} \quad (1)$$

where, *f* represents the proportionality constant (0.42) and *b* is the cell path length (1 cm) (Rakness et al., 2010). The dissolved ozone residual data were then modeled as a first order decay process (Eq. 2), which could then be used to calculate the corresponding ozone exposures (i.e., CT values) using Eq. 3.

$$O_3 \text{ residual [mg/L]} = ((O_3/\text{TOC}) * \text{TOC} - \text{IOD}) * e^{-kt} \quad (2)$$

$$\text{CT [mg-min/L]} = \frac{(O_3/\text{TOC}) * \text{TOC} - \text{IOD}}{k} * (1 - e^{-kt}) \quad (3)$$

where, CT is the ozone exposure (mg-min/L), TOC is the source water concentration of total organic carbon (mg/L), IOD is the instantaneous ozone demand (mg/L), *k* is the first order ozone decay rate constant (min<sup>-1</sup>), and *t* is time (min) (Gerrity et al, 2014).

## 2.4 Methodology for EfOM Characterization with UV Absorbance and Fluorescence

When light of a certain wavelength is passed through a sample, some of the molecules in the sample absorb the light. When photons are absorbed, the absorbing molecule is promoted to an electronically excited state, meaning that the outer electrons transition to a higher energy level. Only a fraction of the incident photons are absorbed by molecules in the solution, and the remaining fraction passes through the solution. Using a spectrophotometer, the intensity of the transmitted radiation (*I*) is compared with that of the incident radiation (*I*<sub>0</sub>), which yields the absorbance or transmittance of the sample (Horiba Scientific, 2012). Wavelength-specific absorbance—typically at 254 nm—is often used as an indicator of water quality. Evaluating

absorbance across the UV spectrum also provides a means of characterizing the organic matter in a sample.

Fluorescence can also be used to assess water quality and characterize organic matter. When the excited electrons eventually relax to their ground state, they release energy in the form of light (i.e., fluorescence). The intensity of the emitted light, which is characterized by a longer wavelength (i.e., less energy) than the incident light, is measured by a spectrofluorometer. These excitation-emission couples can be evaluated across a broad spectrum to generate an excitation emission matrix (EEM), or fluorescence ‘fingerprint’, for a water sample.

For this study, UV absorbance (or transmittance) and fluorescence were determined with a Horiba Aqualog spectrofluorometer (Edison, NJ). Samples were collected from the pilot reactor, brought to room temperature, and filtered using a 0.7- $\mu\text{m}$  GF/F Whatman syringe filter (GE Healthcare Life Sciences, Piscataway, NJ). The analysis settings that were used are provided in Table 1. Data were processed using Matlab (MathWorks, Natick, MA) to generate contour plots of fluorescence emission and intensity (in arbitrary fluorescence units (AFU)) and identify critical fluorescence peaks and regional intensities. The standard operating procedure used for UV<sub>254</sub> and fluorescence determination is provided in Appendix 1.

**Table 1. Raman and sample settings for fluorescence analysis.**

The Raman settings are used to calculate the peak Raman area for a blank sample, which is then used to standardize the fluorescence intensities of experimental samples. That allows for direct comparisons between samples analyzed by different analysts, instruments, labs, etc. The sample settings are used to perform the 3D EEM analysis of samples.

Parameter	Raman	Sample
Integration Period	3 s	3 s
Excitation Wavelength Range	350 nm	240-470 nm
Emission Wavelength Range	380-410 nm	280-570 nm

A Matlab code was used for the evaluation of the fluorescence and UV absorbance as a way to characterize the composition of the samples. The EEMs were divided into three regions. Region I is representative of soluble microbial products (SMPs), region II is associated with fulvic-acid-like substances, and region III is indicative of humic-acid-like substances (Gerrity et al., 2011). An EEM showcasing the three regions can be seen below.

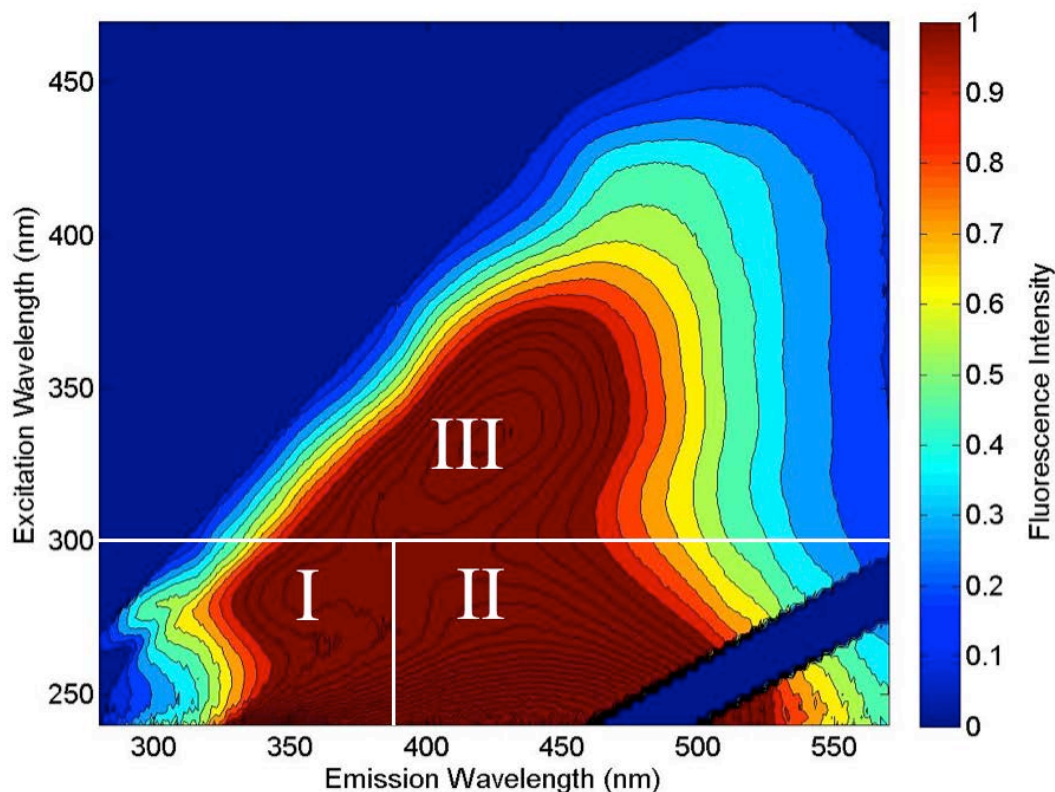


**Figure 3. Fluorescence fractioning for the characterization of EfOM.**

Region I is representative of soluble microbial products, region II is representative of fulvic acids, and region III represents humic acids.

The fluorescence in each region is computed as the volume under the EEM (Zhou, 2013). Fluorescence and fluorophore concentration are directly related (i.e., the higher the fluorescence, the higher the concentration of fluorophores in that region). The fluorescence index (FI) also gives insight into the source of the organic matter. Higher FI values are generally associated with wastewater-derived organic matter due to the presence of soluble microbial products, biopolymers, and proteins, whereas lower FI values are indicative of terrestrially-derived organic matter (Gerrity et al., 2011). The FI compares the fluorescence at emission wavelengths of 450 nm and 500 nm at a constant excitation wavelength of 370 nm.

## 2.5 Methodology for EfOM Quantification based on Total Organic Carbon

A Shimadzu TOC V-csn (Kyoto, Japan) was used for TOC analysis. This instrument measures total organic carbon using the non-purgeable organic carbon (NPOC) method. Acid is added to the sample to decrease the pH and convert inorganic carbon (i.e., carbonate species) to CO<sub>2</sub>, and then the sample is purged with hydrocarbon-free compressed air to eliminate the CO<sub>2</sub>. The sample is then sent to a combustion chamber where the remaining organic carbon is converted to

CO<sub>2</sub> via combustion catalytic oxidation at 680°C. At this point, the CO<sub>2</sub> is sent to a non-dispersive infrared detector and analyzed, and the signals are correlated to TOC concentration. A stock solution using 0.53 g of potassium hydrogen phthalate (KHP) and 250 mL of deionized water was used to produce a 1000 mg/L TOC stock solution. The stock solution was replaced every two months. Standard solutions of 0, 4, 8, 12, 16, and 20 mg/L TOC were prepared using 0, 200, 400, 600, 800, and 1000 µL of stock solution in 50 mL volumetric flasks. These were prepared fresh for each sampling event.

For this study, all glassware were cleaned according to the guidelines provided in Standard Method 5310B. The samples were collected in amber vials (with no headspace), capped with Teflon lined lids, and kept cool prior to analysis. After the samples were acidified using 5N HCl to reduce the pH to less than 2, the samples were covered with parafilm to reduce contamination potential, loaded in the autosampler, and analyzed according to the method parameters provided in Table 2.

**Table 2. NPOC analysis parameter settings for both sample analysis and calibration curve determination.**

Injection Volume	80 µL
Number of Injections	3/7
Standard Deviation Max	0.100
CV Max	3.00%
Number of washes	2
Auto Dilution	1
Sparge Time	1:30 min
Acid Addition	0

## **2.6 Methodology for the Evaluation of Biological Activity based on ATP**

Adenosine triphosphate (ATP) is a compound used by living organisms to store and transfer energy. When ATP reacts with the Luciferase enzyme, light is produced. This light can be measured with a luminometer to determine the concentration of ATP in the sample. The concentration of ATP can be used as an indicator of the presence of bacteria in a system.

A deposit and surface analysis ATP test kit (Hach, Loveland, CO) was used to quantify the biological activity of the biofilm on the biofilter media according to ASTM D4012. This method measures both the intracellular ATP found inside living bacteria as well as ATP dispersed in the sample from decayed biomass.

For ATP analysis, media samples were extracted from the dedicated sample ports on the biofilter columns using sterile scoopulas and stored in sterile sample containers. Control anthracite that had been stored in the refrigerator upon receipt from the San Jose Creek Water Reclamation Plant was also collected to compare with the media from the pilot-scale reactor. One gram of dry

media was added to individual test tubes containing 5 mL of LuminUltra UltraLyse 7, and the tubes were capped. The tubes were inverted several times for mixing and allowed to sit for five minutes to ensure that the ATP was extracted from the lysed bacteria. A 1-mL volume of the resulting liquid (no solids) was transferred to another tube containing 9 mL of LuminUltra UltraLute (for dilution). Prior to analyzing the samples, an ATP standard calibration was performed by adding 100  $\mu$ L of LuminUltra Ultracheck1 and Luminase to a test tube and analyzed using a PhotonMaster Luminometer (LuminUltra Technologies Ltd, New Brunswick, CA). This is done to monitor the luciferase enzyme activity in the Luminase. 100  $\mu$ L of the new solution were transferred to another tube containing 100  $\mu$ L of Luminase. The final sample tube was placed in the luminometer for analysis within 30 seconds.

## 2.7 Nutrient Quantification

Nitrate determination was accomplished with method 8039 (Cadmium Reduction Method) using Hach NitraVer 5 powder pillows. This method measures high range nitrate between 0.3 and 30 mg/L  $\text{NO}_3\text{-N}$ . Nitrite was measured using Method 8507 (Diazotization Method) using Hach NitraVer 3 powder pillows for low range nitrite concentrations (0.002-0.3 mg/L  $\text{NO}_2\text{-N}$ ). Method 10023 (Salicylate Method) for low range ammonia analysis (0.02-2.5 mg/L  $\text{NH}_3\text{-N}$ ) was also used. All of these compounds were measured using a DR5000 spectrophotometer (Hach Corp., USA). For phosphate determination, Method 8048 (Ascorbic Acid) was used with Hach PhosVer 3 powder pillows. Phosphorus was measured using a DR 900 multiparameter handheld colorimeter (Hach Corp., USA).

As will be described later, higher nitrite concentrations were detected in the effluent from the anthracite columns. To determine if any nitrite was originally adsorbed to the media and potentially leaching into the treated water, a leach test was performed on the archived media in the refrigerator. Six samples were evaluated: three crushed samples and three uncrushed samples. A pestle and mortar were used to manually crush the media to very fine particles. A 50 mL test tube was filled with 5.02g of media and filled to the 45 mL mark with distilled water. The samples were allowed to soak for one hour to allow for full saturation of the media. The samples were then placed in a Sorvall Legend RT centrifuge (Thermo Fisher Scientific Inc., USA) for six minutes at 2500 rpm. The supernatant was passed through a 0.7- $\mu$ m filter and analyzed for nitrite.

## 2.8 Total Coliform and *E. coli* Quantification

Standard Method 9223, using IDEXX Colilert-18, was used for total coliform and *E. coli* determination in the pilot reactor samples. This method uses defined substrate technology nutrient indicators ortho-nitrophenyl-  $\beta$ -D-galactopyranoside (ONPH) and 4-methylumbelliferyl- $\beta$ -D-glucuronide (MUG). The  $\beta$ -galactosidase enzyme found in coliform bacteria metabolizes ONPG, producing a yellow color. *E. coli*, on the other hand, uses the  $\beta$ -

glucuronidase enzyme to metabolize MUG, which fluoresces under long-wave ultraviolet light at 366 nm (IDEXX Laboratories, 2015).

For sample analysis, 100 mL of sample was collected in a sterilized, transparent, non-fluorescing IDEXX container containing sodium thiosulfate to quench any residual oxidant present. The samples were collected in triplicate for statistical analysis purposes. The samples were capped and shaken until the sodium thiosulfate dissolved completely. They were then kept cool until the next step could be performed. A Colilert-18 reagent was added to each of the samples and shaken until all nutrients were dissolved. Samples were then transferred to an IDEXX Quanti-Tray/2000 and sealed in an IDEXX Quanti-Tray sealer. The sealed samples were allowed to incubate at 35°C for 18 hours. After incubation, the small and large wells that experienced a color change (yellow) for total coliform or fluorescence for *E. coli* were counted and quantified using the most probable number (MPN) table.

## **2.9 Trace Organic Contaminants**

Due to budget limitations, trace organic contaminants were measured only one time toward the end of the study. Samples of pilot influent, biofiltration effluent (anthracite only), and ozone-biofiltration effluent (ozone-anthracite) were collected in bottles provided by Eurofins Eaton Analytical (Monrovia, CA) and were shipped overnight on ice to the laboratory. Eurofins Eaton Analytical then processed and analyzed the samples for a suite of 94 trace organic contaminants by solid phase extraction, liquid chromatography tandem mass spectrometry (LC-MS/MS), and quantification by isotope dilution. Nine *N*-nitrosamines were also analyzed by the laboratory using EPA Method 521.

## **3.0 Principal Findings and Significance**

### **3.1 Ozone Demand and Decay**

Ozone demand decay curves were generated for O<sub>3</sub>/TOC ratios of 0.5, 1.0, and 1.5 (Figure 4). It was not possible to generate a demand decay curve for the O<sub>3</sub>/TOC ratio of 0.25 because the instantaneous ozone demand (i.e., the demand at 30 seconds) exceeded the transferred ozone dose.

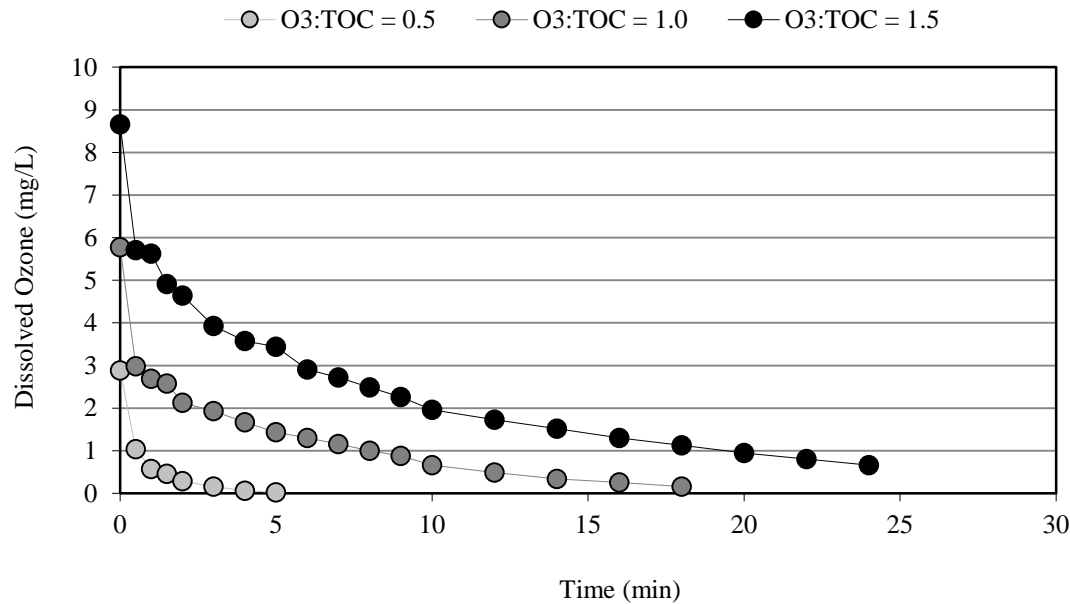


**Figure 4. Ozone demand decay curves for the MBR filtrate as a function of O<sub>3</sub>/TOC ratio.**

The decay witnessed by the ozone is due to a combination of natural ozone decay in pure water and ozone demand from the organic and inorganic compounds in the source water matrix.

The curves indicate the rate at which the ozone decays in this particular water matrix. This gives insight into the composition of the water (i.e., pH, the presence of ozone-reactive organic and inorganic compounds, and the reactivity of those compounds). The extended period of time necessary for complete ozone decay in the presence of 9.5 mg/L of TOC indicates that the bulk organic matter is highly recalcitrant. This is further supported when comparing the pseudo first-order ozone decay rate constants from the study (obtained from performing regressions on the decay curves) versus literature values for similar water matrices (Table 3).

**Table 3. Ozone decay regression and rate constants at different ozone dosing conditions.**

The ozone decay rate constants observed in the study were much lower than the literature values, indicating the presence of ozone resistant compounds in the source water.

O <sub>3</sub> /TOC	Regression	R <sup>2</sup>	Study Rate Constant (min <sup>-1</sup> )	Literature Rate Constant <sup>a</sup> (min <sup>-1</sup> )
0.5	$O_3 = 1.89e^{-0.887t}$	0.98	0.89	1.17-3.78
1	$O_3 = 3.56e^{-0.168t}$	0.98	0.17	0.51-0.83
1.5	$O_3 = 5.68e^{-0.093t}$	0.97	0.09	0.15-0.59

<sup>a</sup>Gamage et al. (2013); four secondary treated wastewater effluents

It is important to note that ozone decay naturally occurs in pure water due primarily to its reaction with OH<sup>-</sup> ions (Staehelin & Hoigné, 1982). The presence of organic matter should increase the ozone rate of decay because of the additional reaction pathways available. According to Staehelin & Hoigné (1982), the rate of decay of ozone in pure water at a pH of 7 is  $1.05 \times 10^{-3} \text{ min}^{-1}$ . Compared with the values in Table 3, this value is significantly smaller. This indicates that the decomposition of ozone that occurred during the demand/decay test is

representative of the reaction between ozone and the source water matrix and not due to natural decomposition alone.

### 3.2 Nutrient Removal

Nutrient removal was monitored over a two-month period for the anthracite columns (C1-C4 and the control) with preozonation and for the BC column without preozonation. Ammonia, nitrate, nitrite, and phosphate were monitored. Nitrate and nitrite concentrations for the anthracite columns were aggregated due to their values, and the averages were plotted alongside the concentrations of the reactor influent and BC effluent (Figures 5 and 6).

Influent concentrations of ammonia, nitrate, and nitrite were low because of the nitrification and denitrification achieved by the full-scale MBR. In fact, ammonia concentrations were negligible in all samples. Nitrate concentrations in the reactor influent (i.e., MBR filtrate) varied from  $<0.3$  to  $\sim 10$  mg-N/L; the biofiltration effluent typically exhibited similar concentrations. Although the BC contains denitrifying bacteria, the performance of these bacteria is dependent on having low dissolved oxygen levels and a sufficient carbon source to serve as the electron donor. During this phase of testing, the feed to the BC column was non-ozonated effluent, which limited the dissolved oxygen level in the feed water, but there was still 3.3 mg/L of dissolved oxygen present. More importantly, there was an inadequate carbon source to drive the denitrification process. On the other hand, the anthracite columns likely had a sufficient carbon source to drive the process, but the supersaturated dissolved oxygen levels inhibited the denitrification pathway. No phosphate removal was witnessed through the biofilters, and the phosphate concentrations in the reactor influent (i.e., MBR filtrate) were highly variable (data not shown).

One interesting observation was a consistent accumulation of nitrite in the anthracite columns, as shown in Figure 6. This nitrite accumulation did not occur in the BC column, however. The anthracite media was evaluated to determine if nitrite leaching was occurring. The average nitrite concentrations obtained from the uncrushed and crushed media were  $0.001 \pm 0.004$  mg-N/L and  $0.007 \pm 0.004$  mg-N/L, respectively. These concentrations are extremely low and indicate that the higher nitrite concentrations observed were not due to leaching from the media. One possible explanation is the presence of micro-communities within the larger biofilter community. Although high influent dissolved oxygen concentrations were supplied to the anthracite filters, it is possible that small portions of the filter developed anoxic conditions, thereby supporting the conversion of nitrate to nitrite. Although no significant nitrate removal was observed, the low levels of nitrite witnessed would not require substantial nitrate transformation. Once the nitrite was formed, it is possible that an inadequate supply of carbon limited nitrite conversion to nitrogen gas. A study by Liu et al. (2006) documented high levels of denitrification intermediates, such as nitrite, in biofilter effluent due to low concentrations of electron donors. Other sources also cite an inadequate supply of organic matter as the reason for residual nitrite in biofilters (Sison et al., 1995; Sison et al., 1996).

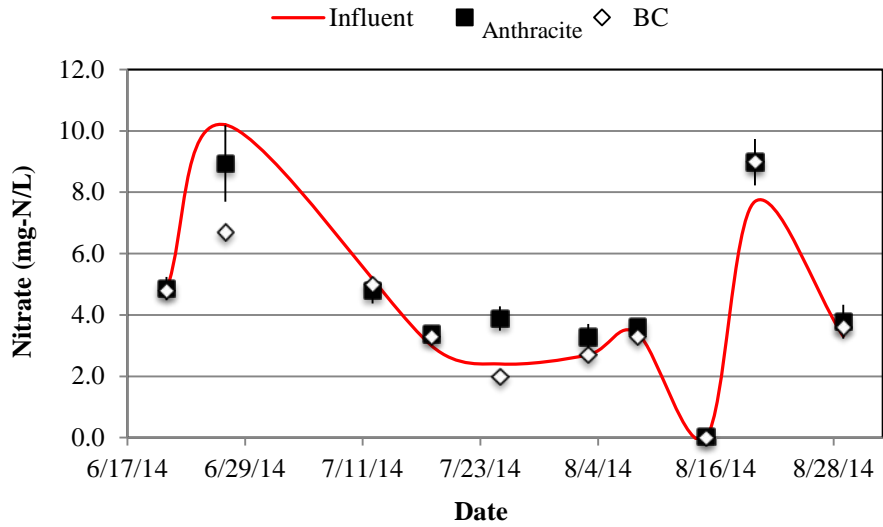


**Figure 5. Nitrate concentrations in the influent and biofilter effluents.**  
 The anthracite data represent average concentrations ( $\pm 1$  standard deviation) based on aggregated data from all of the columns.

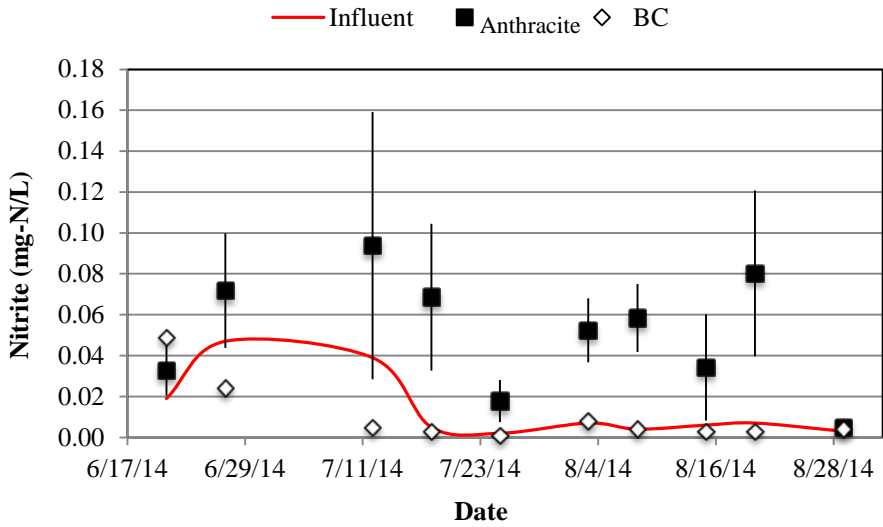


**Figure 6. Nitrite concentrations in the influent and biofilter effluents.**  
 The anthracite data represent average concentrations ( $\pm 1$  standard deviation) based on aggregated data from all of the columns. The anthracite columns consistently exhibited higher nitrite concentrations than the influent or BC effluent.

### 3.3 TOC Removal with Ozone-Biofiltration

#### 3.3.1 UV<sub>254</sub> and O<sub>3</sub>/TOC Correlation

Based on data obtained from the ozone demand/decay test, a correlation between UV<sub>254</sub> and ozone dose was developed (Figure 7). The correlation was consistent with similar correlations

presented in the literature (Gerrity et al., 2012). The corresponding regression equation was used to estimate the transferred ozone doses during the kinetics testing (Section 3.3.3).

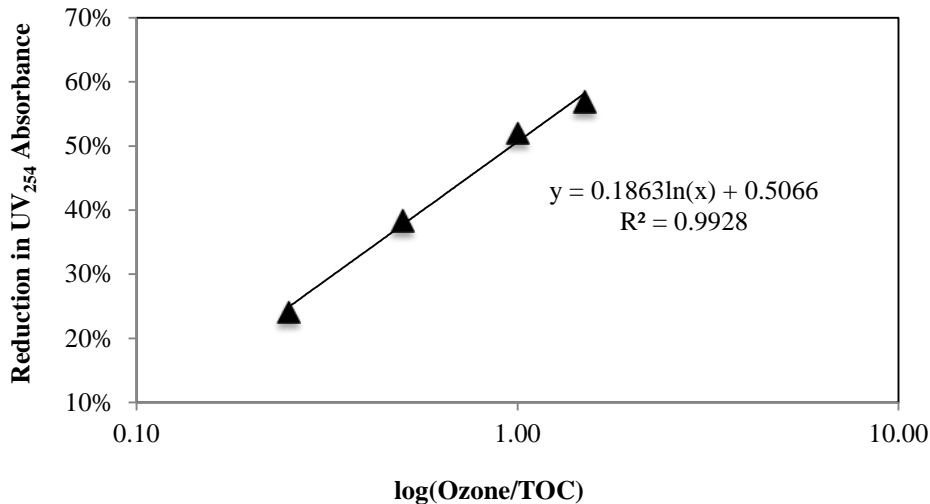


**Figure 7. Relationship between O<sub>3</sub>/TOC and reductions in UV<sub>254</sub> absorbance.**  
Data from the ozone demand/decay testing was used to develop the relationship.

### 3.3.2 Long-Term Testing of Ozone-Biofiltration

The initial hypothesis of the study was that by providing higher ozone doses and longer empty bed contact times, ozone-biofiltration systems could achieve lower effluent TOC concentrations. In practice, the benefits of longer empty bed contact times (e.g., greater reductions in TOC) have been demonstrated in full-scale ozone-BAC systems in Australia, which employed empty bed contact times ranging from 9 – 45 minutes (Reungoat et al., 2012). However, the feed water and ozone doses differed at each plant so it is difficult to determine whether the extent of TOC removal was primarily impacted by EBCT. Therefore, the current study targeted a more controlled experiment by evaluating the impacts of varying EBCT in parallel columns.

As mentioned earlier, ozonation was required to initiate growth of the microbial community on the filter media. Prior to ozonation, limited TOC removal (~5%) was observed through the biofilters, thereby indicating minimal adsorption and biodegradation, but after initiation of the ozone process, TOC removal in the biofilter effluent increased rapidly (Figure 8). It is important to note that there was an insignificant level of TOC removal due to ozonation alone, thereby indicating that biodegradation in the biofilters was the dominant mechanism responsible for reductions in TOC. Once the TOC removal (and presumably the microbial community) had stabilized, the EBCTs were set at values ranging from 5 – 15 minutes, as described in Section 2.1.3, and the ozone dose was maintained at a relative low O<sub>3</sub>/TOC ratio of ~0.35.

Based on the performance of the full-scale ozone-BAC systems in Australia, higher EBCTs should result in lower effluent TOC concentration. Despite the range of EBCTs, the TOC removal through the biofilters receiving ozonated water was relatively constant at ~15% (Figure 9), even for the BC. Coupled with the conclusion from the ozone demand/decay testing that the

MBR filtrate was recalcitrant, the revised hypothesis was that the low ozone dose was unable to generate a sufficient concentration of biodegradable organic matter to necessitate EBCTs longer than ~5 minutes. As a result, the experimental approach shifted from long-term operation at a range of EBCTs to short-term kinetics testing at lower EBCTs and with greater time resolution.

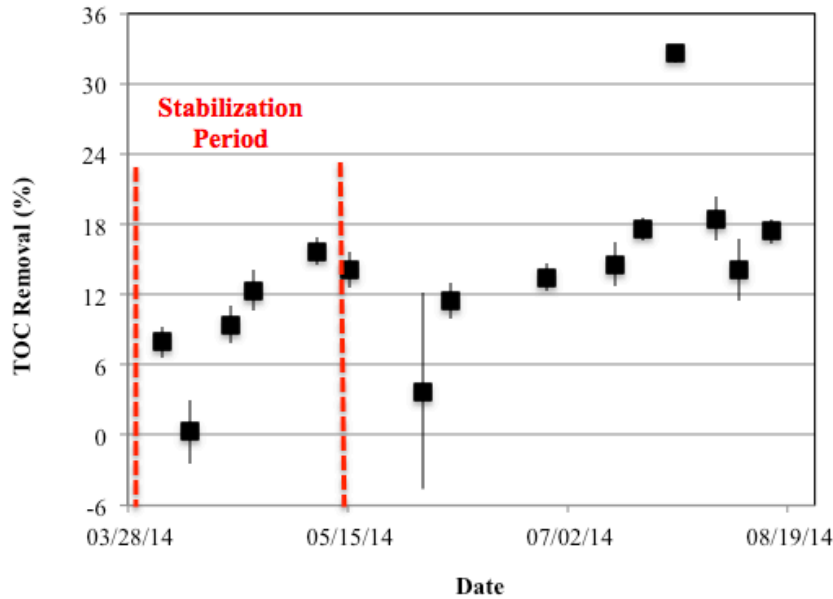


**Figure 8. TOC removal in the anthracite and BC biofilters after initiation of the ozone process.** The data represent average concentrations ( $\pm 1$  standard deviation) based on aggregated data from all of the columns receiving ozonated water. The relatively low TOC removal observed in late May 2014 was attributed to an operational upset in the ozone contactors.

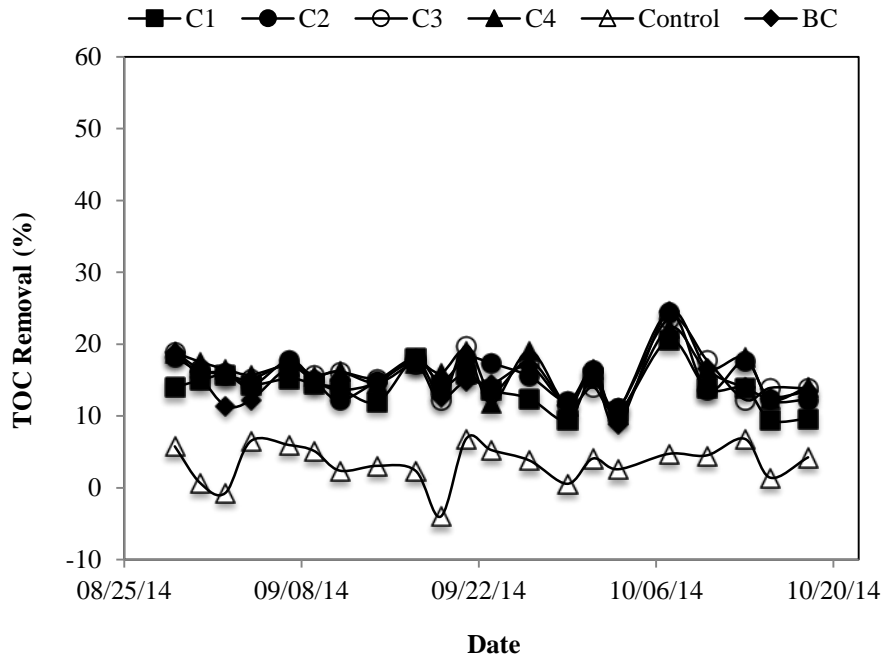


**Figure 9. TOC removal in the anthracite and BC biofilters with varying EBCTs.** The EBCTs were as follows: C1=5 min, C2=10 min, C3=10 min, C4=15 min, Control=10 min, and BC=10 min. During this phase of testing, all columns except the BC contained anthracite, and all columns except the Control were receiving ozonated feedwater.

### 3.3.3 Kinetics Tests Results

Three kinetics tests were performed for this study with each test targeting a different O<sub>3</sub>/TOC ratio. During the long-term operational testing phase, an average reduction in UV<sub>254</sub> absorbance of 30% (O<sub>3</sub>/TOC of 0.35) was achieved; therefore, this setting was used for the first kinetics test. The second test targeted the highest achievable reduction in UV<sub>254</sub> absorbance (based on the limitation of the ozone generator), which was about 50% or an estimated O<sub>3</sub>/TOC of 1.12. Lastly, kinetics test 3 achieved an average reduction in UV<sub>254</sub> absorbance of 40% (O<sub>3</sub>/TOC of 0.62). It should be noted that the only samples collected during the kinetics tests were influent, C2 (ozone+anthracite), C3 (ozone+exhausted GAC), control (anthracite), and effluent (ozone). Due to the complexity of the operational and sampling procedures, it was not feasible to collect samples from C1 (ozone+anthracite) and C4 (ozone+anthracite). Due to severe compaction of the polyvinyl alcohol biobeads experienced with the BC, the flow rate was extremely low and could not be adjusted to flow rates necessary for the tests. Therefore, the BC column was decommissioned for the duration of the project.

The effect of the changing ozone dose can be seen in Figure 10, which illustrates changes in fluorescence. Humic-like substances (Region III; refer to Figure 3) were considerably reduced with an O<sub>3</sub>/TOC of 0.35, biopolymers experienced a significant decrease in fluorescence with an O<sub>3</sub>/TOC of 0.62, and fulvic-like substances were significantly transformed at an O<sub>3</sub>/TOC of 1.12. As indicated visually in Figure 10 and quantitatively in Table 4, increasing ozone doses improve water quality in all regions and yield EEMs that are more consistent with natural surface waters. Therefore, ozone is effective in eliminating the ‘wastewater identity’ of the matrix, which is critical for public perception in potable reuse applications. This is supported by the reduction in the FI between the influent and ozonated effluent samples (Table 4), which corresponds with reductions in microbially-derived organic matter in region I.

**Table 4. EfOM characterization at different ozone doses**

Increasing the ozone dose resulted in reductions in fluorophores in all regions and a reduction in FI from the influent to ozonated effluent samples.

Sample	O <sub>3</sub> /TOC	Region I	Region II	Region III	Total Fluor.	TF Removal (%)	FI
Inf	0.00	18,305	24,792	12,289	55,386	--	1.91
Eff	0.35	5,214	6,200	2,437	13,851	75	1.37
Inf	0.00	16,827	20,627	9,122	46,577	--	1.70
Eff	0.62	2,517	3,930	1,453	7,900	83	1.41
Inf	0.00	13,965	17,206	8,154	39,325	--	1.76
Eff	1.12	576	1,381	615	2,572	93	1.46

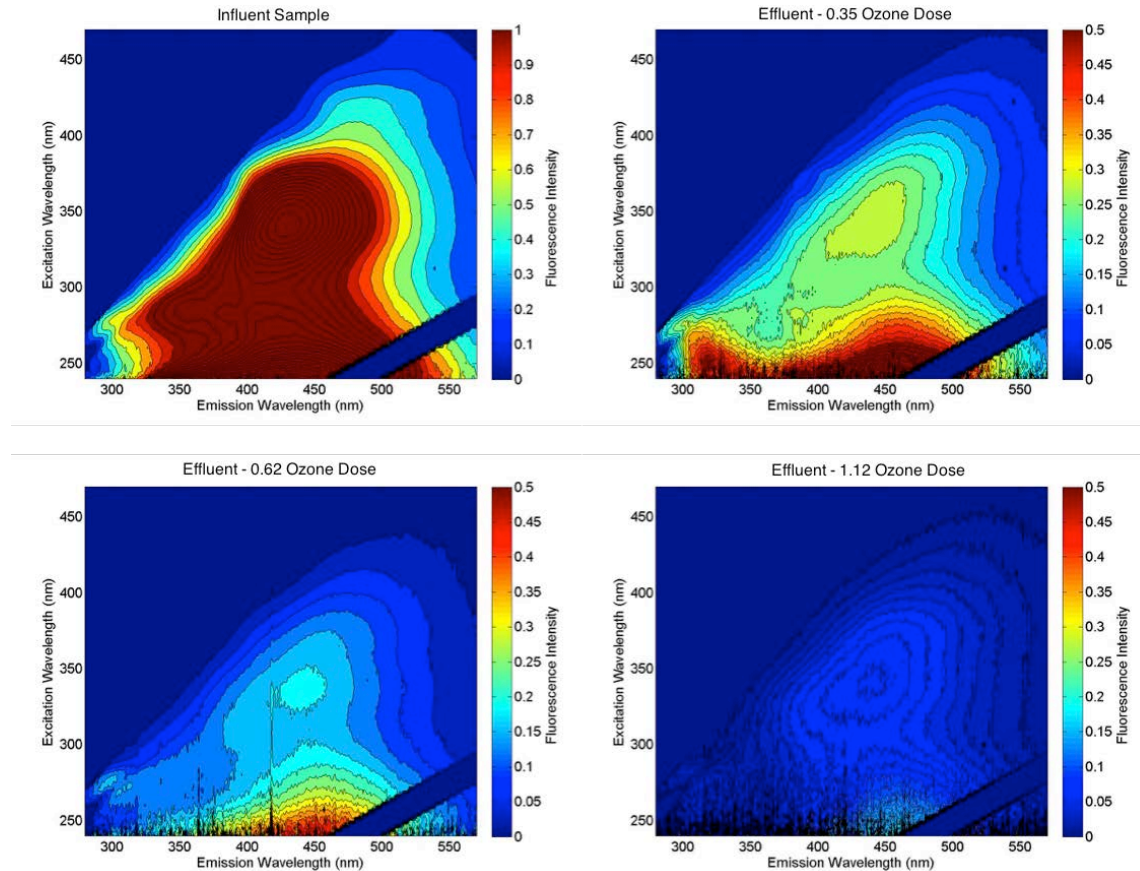


**Figure 10. EEM comparison of three ozone doses.**

The changes in the fluorescence intensity of the EEM are indicative of the level of organic matter transformation from ozone oxidation. As the ozone dose increases, the more recalcitrant compounds are oxidized, and the number of fluorescing compounds is reduced. *Note the change in scale from the influent to the effluent samples, which increases the resolution of the treated EEMs.*

The results of kinetics test one ( $O_3/TOC=0.35$ ) are provided in Figure 11. A positive correlation can be seen between TOC removal and EBCT up to around six minutes of contact time. After six minutes, little improvement is observed with increasing contact time. This is consistent with the observed performance of the biofilters during the long-term testing phase with EBCTs ranging from 5 – 15 minutes. It is important to reiterate that C3 contained exhausted GAC (or BAC) during this phase of testing. Therefore, C2 and C3 provide a direct comparison of anthracite and exhausted GAC for ozonated feedwater, and C2 and the control provide a direct comparison of ozonated vs. non-ozonated feedwater with anthracite as the surface for biofilm attachment. Based on the results of this initial test, the anthracite and exhausted GAC performed similarly, while the control column receiving non-ozonated effluent exhibited inferior performance. The performance of the control column was consistent with the start-up period for all columns prior to initiation of the ozone process and the initial long-term testing of varying EBCTs.

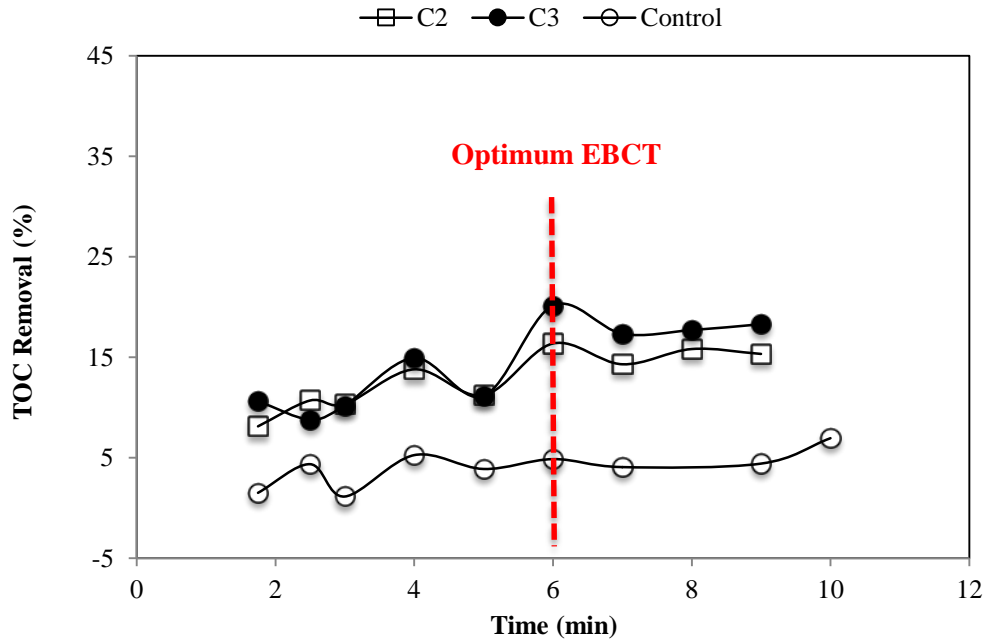


**Figure 11. Kinetics test one (O<sub>3</sub>/TOC=0.35) results for TOC removal at various EBCTs**

Kinetics test two was performed at an O<sub>3</sub>/TOC of 1.12. The same trend observed in the first kinetics test was also apparent at this higher ozone dose. However, the additional ozone led to greater TOC removal through the columns, as indicated in Figure 12. Also, the contact time after which the TOC removal stabilized increased from six minutes to ~10 – 12 minutes.

The final kinetics test was performed using an intermediate O<sub>3</sub>/TOC of 0.62. Again, the results are similar to the previous kinetics tests, as seen in Figure 13. As expected, based on tests 1 and 2, the TOC removal stabilized at an intermediate contact time of nine minutes, assuming the large fluctuations at higher EBCTs were attributable to experimental error/variability rather than operational performance. The experimental error/variability assumption is supported by the similar trends observed for all three media, but it is unclear what caused this effect.

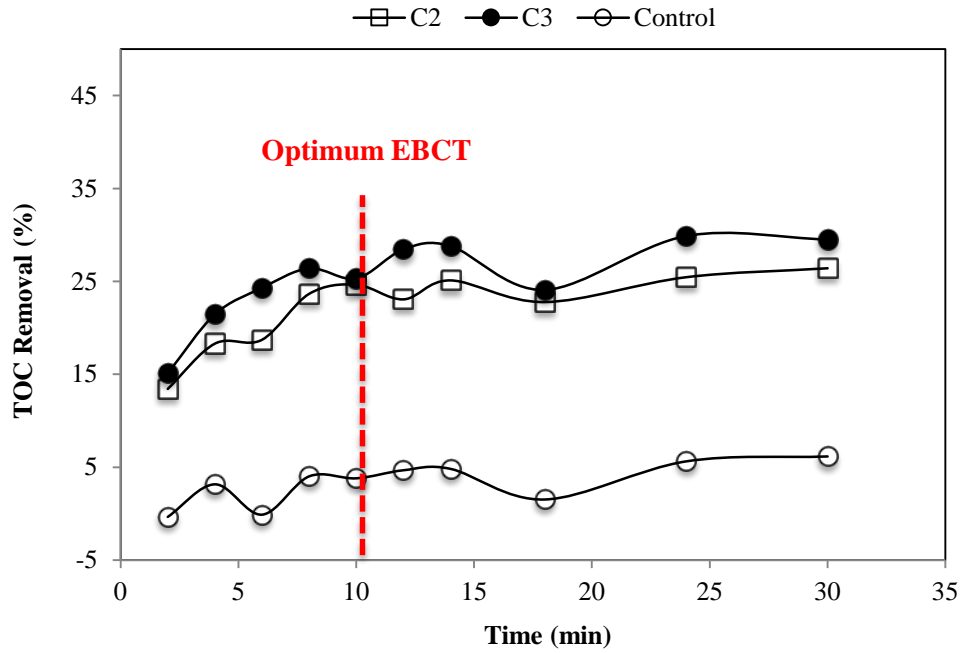


Figure 12. Kinetics test two ( $O_3/TOC=1.12$ ) results for TOC removal at various EBCTs

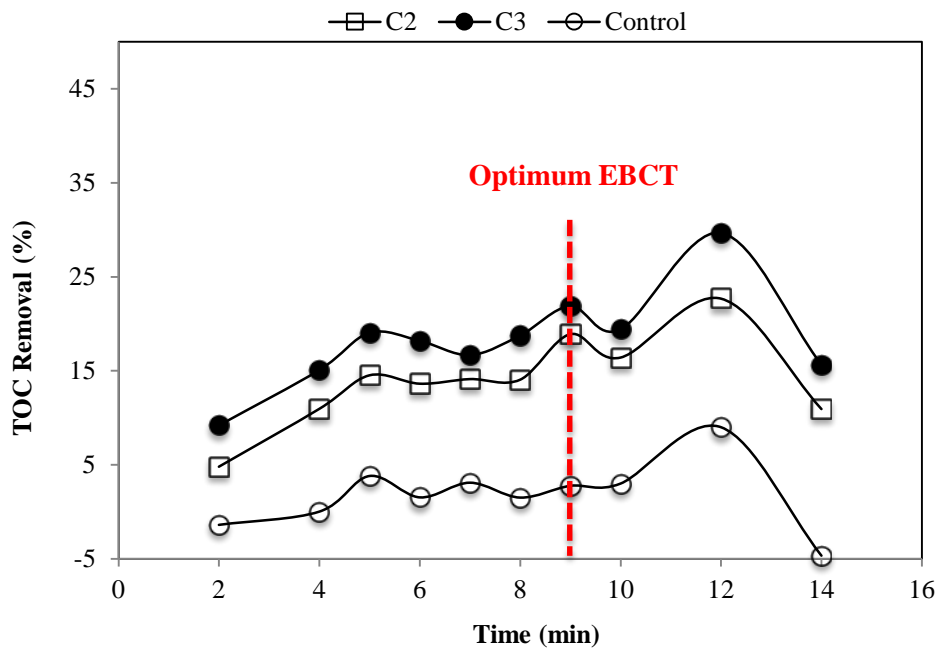


Figure 13. Kinetics test three ( $O_3/TOC=0.62$ ) results for TOC removal at various EBCTs

It can be seen that higher ozone doses lead to greater reductions in TOC during biofiltration, as would be expected. Kinetics test 2, which had the highest ozone dose ( $O_3/TOC=1.12$ ), provided the best treatment for both biofilters evaluated. The exhausted GAC generally exhibited better performance than the anthracite, although the differences were small, while the control anthracite column consistently achieved reductions in TOC of less than 5%.

Each kinetics test was examined individually to determine the optimum EBCT at the specific ozone dose. These points were chosen through graphical observation of the point of diminishing return, or the time after which little improvement in treatment efficacy is observed. Providing additional contact time with little treatment enhancement would have negative consequences to a full-scale system; longer retention times equate to lower flow rates or greater structural footprints and higher costs per unit of water treated. These results are tabulated in Table 5.

**Table 5. Comparison of optimum conditions and treatment efficacy.**

$O_3/TOC$	Optimum EBCT	TOC Removal (1.2-mm Anthracite)	TOC Removal (0.95-mm Exhausted GAC)	Minimum TOC Achieved
	minutes	%	%	mg/L
0.35	6	16	20	6.4
0.62	9	19	22	5.7
1.12	10 – 12	25	25	5.0

If higher ozone doses were used, it is possible that the minimum TOC values could be reduced even further (i.e., more extensive transformation of bulk organic matter and greater removal of TOC after biodegradation). Unfortunately, due to constraints with the ozone generator, this was the highest achievable ozone dose. Based on Table 5, it appears that a relationship exists between ozone dose and optimum EBCT. To evaluate this potential relationship, the two parameters were graphed against each other and analyzed. The relationship between ozone dose and EBCT is illustrated in Figure 14. A logarithmic function provides some estimation of the relationship, but additional data are clearly warranted to further validate the model. Interestingly, the current data suggest a point of diminishing return for the combination of ozone and EBCT; in other words, there may be a limit to the practical extent of transformation and the generation of biodegradable organics that ultimately serve as food for the microbial community.

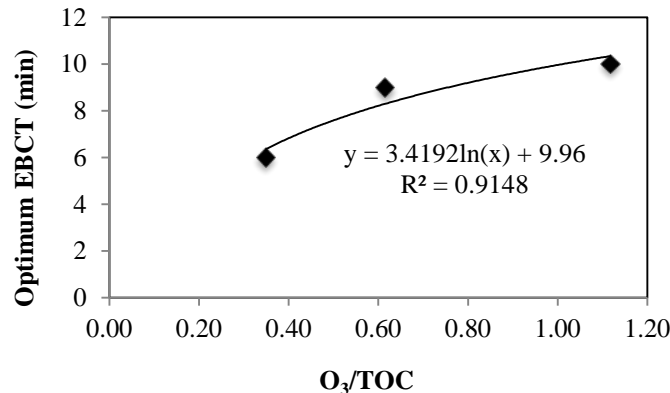


**Figure 14. Relationship between ozone dose and optimum EBCT.**

### 3.4 ATP Testing

It is evident from the kinetics tests that C3 (ozone+0.95 mm diameter exhausted GAC) outperformed C2 (ozone+1.2 mm diameter anthracite) at every ozone dose. There are two potential explanations for this observation: (1) the smaller media provides more surface area for biological growth or (2) the smaller media is better suited for the column size and enhances the hydraulic efficiency of the filter. To evaluate these theories, ATP concentrations corresponding to attached growth on the various media were analyzed at three different times during the study (Tables 6 – 8). Table 6 summarizes the ATP concentrations for the initial start-up period while the columns were receiving non-ozonated effluent and minimal TOC removal was observed. Values from the literature are also provided as a basis for comparison. Table 7 summarizes the ATP concentrations for the various columns after they had been receiving ozonated feedwater for six months. At the time of collection, the control column had been receiving non-ozonated feedwater for approximately one month, but it had received ozonated feedwater for five months prior to promote biological growth. Conversely, the BC had been receiving ozonated feedwater for approximately one month, but it had received non-ozonated feedwater for several months prior. Finally, Table 8 provides a comparison of the data from Table 7 and a subsequent sample event approximately 6 months later.

Tables 6 – 8 illustrate the development of the microbial communities over time, particularly following the initiation of the ozone process. The ATP concentrations increased several orders of magnitude following ozone start-up, at which point they were more consistent with values reported in the literature (Table 6). With respect to media depth, Table 8 indicates that both C2 and C3 exhibited significantly higher ATP concentrations at the top of the filter. Furthermore, the ATP concentration at the bottom of the filter exhibited a greater relative decline for the smaller media. This could be linked to more rapid depletion of available organic substrate at the top of C3, which might have hindered biological growth lower in the column.

The higher ATP concentration at the top of C3 versus C2 (Table 8) might be linked to media size (i.e., higher specific surface area of the smaller GAC media) and biofilter performance. Additional biological growth may have contributed to the superior performance of C3, but it cannot be stated absolutely because the potential impact of hydraulic inefficiency was not evaluated. It is also interesting to note that once bacteria colonized the control media when it was originally fed with ozonated water, the high levels of ATP persisted despite the fact that the column was transitioned to non-ozonated effluent at the end of the study. Therefore, the organic matter proved to be too recalcitrant to promote significant reductions in TOC, but it was sufficient to maintain the biomass in the system. Alternatively, the biomass may have become dormant or inactivated, but the ATP test still detected the residual cellular materials present on the media.

It was also observed that the BC had significantly higher ATP concentrations, but there was no appreciable improvement in biofilter performance. The same level of treatment was achieved with C2, which had much less ATP than the BC. Moreover, better treatment was witnessed in C3, which also exhibited a lower ATP concentration. This further proves that higher biomass concentrations do not always equate to more biological activity as measured by TOC removal, which has been stated in previous publications (Pharand et al., 2014). The higher ATP

concentration for the BC may have been attributable to ATP originating from inside the biobeads, whereas the anthracite and exhausted GAC could not support growth within their internal structures. Diffusion limitations may have negatively impacted the ability of the internal biomass to degrade the bulk organic matter in the BC column.

**Table 6. Summary of the initial ATP analysis of the anthracite compared against ATP data from the literature.**

Prior to ozonation, the ATP concentrations found on the anthracite in the study were significantly lower than typical literature values. This indicates the gross underdevelopment of the biological community in the biofilters prior to start-up of the ozone process. C3 had not been switched to exhausted GAC at this point in the study.

Media Sample	Sample Source	ATP (pg ATP/g media)	Reference
Stored Anthracite	Refrigerator	$0.6 \times 10^2$	Current Study
C1 (anthracite)	Bottom of Contactor	$6.6 \times 10^2$	Current Study
C3 (anthracite)	Bottom of Contactor	$2.3 \times 10^2$	Current Study
Control (anthracite)	Bottom of Contactor	$2.9 \times 10^2$	Current Study
Literature	75-day old GAC	$1.8 \times 10^6$	Velten et al., 2007
Literature	90-day old GAC	$8.0 \times 10^5 - 1.8 \times 10^6$	Velten et al., 2011
Literature	30 GAC filters from 9 WWTPs	$1.4 \times 10^4 - 2.5 \times 10^5$	Magic-Knezev, 2004

**Table 7. Summary of ATP concentrations six months after start-up of the ozone process.**

Relative to the data in Table 6, the ATP concentrations increased by several orders of magnitude after the feedwater was ozonated. C3 had not been switched to exhausted GAC at this point in the study. At the time of sampling, the control anthracite was receiving non-ozonated feedwater, but it had been receiving ozonated feedwater for 5 months prior.

Media Sample	Sample Location	ATP (pg ATP/g media)
C1 (anthracite)	Bottom	$0.34 \times 10^6$
C2 (anthracite)	Bottom	$0.20 \times 10^6$
C3 (anthracite)	Bottom	$0.30 \times 10^6$
C4 (anthracite)	Bottom	$0.14 \times 10^6$
Control (anthracite)	Bottom	$0.06 \times 10^6$
Biocatalyst	Top	$2.00 \times 10^6$
Stored Biocatalyst	Refrigerator	$0.31 \times 10^6$

**Table 8. ATP concentrations at two biofilter depths over time and as a function of media type.**

ATP concentrations were higher at the top of the columns. The 0.95 mm exhausted GAC exhibited a higher concentration than the 1.2 mm anthracite, which may be due to the larger specific surface area of the smaller media.

Sample	tATP at Top of Column (pg ATP/g media)		tATP at Bottom of Column (pg ATP/g media)	
	9/10/14	3/24/15	9/10/14	3/24/15
C2 (O <sub>3</sub> /anthracite)	--	$0.63 \times 10^6$	$0.20 \times 10^6$	$0.31 \times 10^6$
C3 (O <sub>3</sub> /BAC)	--	$0.91 \times 10^6$	--	$0.22 \times 10^6$
Control (No O <sub>3</sub> /anthracite)	--	--	$0.06 \times 10^6$	$0.20 \times 10^6$
Biocatalyst (O <sub>3</sub> /biocatalyst)	$2.0 \times 10^6$	$2.3 \times 10^6$	--	--

\*Dashes represent samples that were not collected

### 3.5 Total Coliform and *E. coli* Evaluation

One of the concerns associated with biofiltration is the reintroduction of bacteria into the water. Considering that the water might ultimately be used for potable reuse applications, *E. coli* are also relevant in terms of compliance with U.S. EPA drinking water regulations. Samples were collected for the reactor influent (MBR filtrate), effluent (ozone only), C2 (ozone+anthracite), and the control column (anthracite only), and the results are provided in Table 9. All samples tested negative for *E. coli*. There was a small amount of total coliform bacteria present in the influent water. Theoretically, there should be no coliform bacteria present in the influent water because it is MBR filtrate, and the pore size of the membrane is smaller than the size of bacteria. The presence of coliform bacteria may be attributable to growth in the system tubing connecting the MBR sample port to the pilot reactor as well as growth within the reactor components. In fact, noticeable growth was observed in the static mixer located upstream of the influent sample port. Once ozonated, all of the coliform bacteria in the water were inactivated, as indicated by the ozone effluent values. Also, no coliform bacteria were present in the C2 effluent, which indicates that regrowth and release of coliform bacteria did not occur in the ozone-anthracite column (at least during this sample event). Interestingly, the control column had the highest number of coliform bacteria—even higher than the influent. This means that some of the biofilm may have been detaching from the media and entering the water. This suggests that the addition of ozone may not only aid in biofilm growth but also in biofilm attachment to the media or the selection of bacterial species other than coliform bacteria. The issue of microbial, specifically pathogen, regrowth and release into the final product water could potentially be problematic in full-scale operations and would warrant a final disinfection process downstream of the biofilters. Regardless of the regrowth potential, recent regulatory frameworks for potable reuse would likely necessitate a final disinfection process to achieve specified levels of inactivation and/or removal of target pathogens (NWRI, 2013).

**Table 9. Total coliform bacteria in the pilot system.**

The total coliform concentration increased through the control column, which suggests detachment of the biofilm into the water. Ozone was effective at inactivating coliform bacteria resulting in <1 MPN/100 mL in the ozonated effluent and C2 effluent.

Sample	Total Coliform (MPN/100 mL)			
	1	2	3	Average
Influent	8.5	3.1	6.3	6.0±2.7
C2	<1	<1	<1	<1
Control	13.4	14.5	8.6	12.2±3.1
Effluent	<1	<1	<1	<1

### 3.5 Trace Organic Contaminant Mitigation

Only 33 of the 103 trace organic contaminants (TOrcs) and nitrosamines monitored in this study were detected in either the pilot influent, control (anthracite only) effluent, or C2

(ozone+anthracite) effluent (Table 10). Some TOrcs were removed by biofiltration alone (e.g., the antibiotics amoxicillin, sulfamethoxazole, and trimethoprim), but others (e.g., the artificial sweetener acesulfame-K) actually increased during biofiltration. The combination of ozone and biofiltration proved to be effective in reducing the concentrations of many TOrcs, and only 21 of the 103 target compounds were detected in the ozone-biofiltration effluent. The literature suggests that the vast majority of these compounds pose no threat to public health at these low concentrations. One exception is *N*-nitrosodimethylamine (NDMA), which has a 10-ng/L notification level in California. The concentration of NDMA was actually <MRL in the effluent from the control column, but it was 12 ng/L in the ozone-anthracite effluent. Some studies have reported significant formation of NDMA during ozonation of wastewater effluents (Gerrity et al., 2014), and post-ozone biofiltration has been shown to reduce NDMA concentrations (Gerrity et al., 2015). Additional testing would be necessary to determine if ozone-induced NDMA formation would be an issue in this particular matrix and whether the biofiltration process could be used to reduce NDMA concentrations. Regardless, the potential for NDMA exceedances would necessitate further treatment to consistently comply with the notification level.

**Table 10. Summary of trace organic contaminant concentrations (ng/L) in the reactor influent, biofiltration (anthracite only) effluent, and the ozone-biofiltration (ozone-anthracite) effluent.**

Target Compound	Influent	Biofiltration	Ozone-Biofiltration	Target Compound	Influent	Biofiltration	Ozone-Biofiltration
Acesulfame-K	570	1500	730	Isobutylparaben	<5	8.1	<5
Albuterol	34	<5	<5	Lidocaine	450	410	<5
Amoxicillin	3100	1800	<20	Linuron	10	15	<5
Atenolol	370	68	17	Meprobamate	36	36	44
Bisphenol A	25	270	190	Naproxen	<10	30	16
Butalbital	<5	76	53	NDEA <sup>2</sup>	<2	2	<2
Caffeine	29	<5	<5	NDMA <sup>3</sup>	9.9	<2	12
Carbamazepine	74	70	<5	NMOR <sup>4</sup>	2.8	5.2	3
Cotinine	64	41	46	Primidone	220	200	61
DEET <sup>1</sup>	41	49	12	Sucralose	22000	23000	23000
Dehydronifedipine	7.5	6.4	5.6	Sulfamethoxazole	810	530	13
Diclofenac	<5	160	130	TCEP <sup>5</sup>	96	69	78
Diltiazem	82	35	<5	T CPP <sup>6</sup>	920	800	620
Erythromycin	77	86	<10	TDCPP <sup>7</sup>	240	4900	230
Fluoxetine	20	<10	<10	Triclosan	<10	13	15
Gemfibrozil	<5	36	12	Trimethoprim	160	38	<5
Iohexal	980	2200	730				

<sup>1</sup>*N,N*-diethyl-meta-toluamide, <sup>2</sup>*N*-nitrosodiethylamine, <sup>3</sup>*N*-nitrosodimethylamine, <sup>4</sup>*N*-nitrosomorpholine, <sup>5</sup>tris(2-chloroethyl)phosphate, <sup>6</sup>tris(1-chloro-2-propyl)phosphate, <sup>7</sup>tris(1,3-dichloro-2-propyl)phosphate.

\*Shading represents compounds that were present at concentrations lower than their method reporting limits (MRLs). 100 additional target compounds were <MRL in all samples so they were omitted from the summary table.

## 4.0 Conclusions

This study evaluated the performance of an ozone-biofiltration pilot reactor using anthracite, exhausted GAC (or BAC), and a proprietary biocatalyst as the filter media. Biological growth was monitored based on TOC removal and ATP concentrations. Once a stable biological community was established, enhanced TOC removal was evaluated by increasing ozone dose and/or EBCT. Based on the results of the study, several conclusions can be made regarding ozone-biofiltration system performance and recommendations for operational conditions.

#### **4.1 Findings Confirming Previous Work**

- Up to 92% of the humic-like substances were transformed through ozonation, with an additional 2% reduction provided through biofiltration. In addition, there was minimal reduction in TOC during ozonation but a substantial reduction in TOC during biofiltration. Therefore, fluorescence and TOC are complementary bulk organic parameters for evaluating the ozone and biofiltration performance, respectively, of ozone-biofiltration treatment trains.
- A logarithmic relationship was identified between  $UV_{254}$  removal and  $O_3/TOC$ , which allows for estimation of ozone dosing based on changes in  $UV_{254}$  absorbance. A similar relationship could be developed for changes in fluorescence, but fluorescence was not monitored during the ozone demand/decay test in this study.
- Higher ozone doses yielded better reductions in TOC,  $UV_{254}$  absorbance, and fluorescence when coupled with biofiltration.
- ATP concentrations were higher at the top of the biofilters as compared with the bottom of the biofilters. The small media provided more surface area for biological growth, which potentially explains the higher ATP concentration per gram of small media. This may also explain the better treatment efficacy achieved with the small media, although hydraulic performance may also be a contributing factor.
- The biocatalyst housed the highest concentration of ATP (~50% more ATP) but did not yield additional TOC removal. This suggests that higher biofilm concentrations do not necessarily correlate with better treatment in all applications.

#### **4.2 Significant Findings of this Study**

- The anthracite biofilters were unable to remove  $NO_3-N$ ,  $NO_2-N$ , and  $PO_4-P$  from the water and actually contributed to higher nitrite concentrations in the treated water. The biocatalyst did not experience the same increase in nitrite, but it was unable to achieve reductions in nitrate, despite the fact that it contained denitrifying bacteria. However, the biocatalyst is intended for suspended growth systems—not packed bed configurations. In addition, the supersaturated dissolved oxygen conditions after ozonation are not conducive to denitrification. Therefore, additional testing of the biocatalyst with more appropriate operational conditions is recommended. In fact, denitrification will be crucial in potable reuse applications because of the 10 mg-N/L maximum contaminant level (MCL) for nitrate in drinking water. The full-scale MBR was able to achieve the

nitrate MCL without additional treatment, but other biological treatment systems may not have such an effective denitrification process. Therefore, the use of a denitrifying biocatalyst might be advantageous if it can be effectively integrated into ozone-biofiltration systems.

- No *E. coli* was found at any point in the system, but total coliform bacteria were discovered in the influent and control effluent. The control exhibited higher total coliform numbers than the influent, which suggests that the biofilm may have detached from the media and entered the water. The ozonated column, however, did not contribute any coliform bacteria despite the higher ATP concentration present. This suggests that ozonation may impact biological attachment to the media or it may select for different species of bacteria due to the change in biodegradable organic matter.
- One of the major objectives of the study was to identify a relationship between ozone dose and empty bed contact time for TOC removal. Based on the kinetics tests performed, optimum EBCTs for various ozone doses were identified. The optimum EBCTs for O<sub>3</sub>/TOC of 0.35, 0.62, and 1.12 were found to be 6, 9, and 10 – 12 minutes, respectively. These EBCTs are significantly lower than what is used in some full-scale facilities so it is unclear whether EBCTs of up to 45 minutes are actually warranted. When plotting optimum EBCT versus O<sub>3</sub>/TOC, a logarithmic relationship appeared to exist between the two parameters. Based on this relationship, it appears that relatively low EBCTs are necessary for TOC removal. However, additional testing is warranted to validate the relationship and determine whether water quality (e.g., MBR filtrate vs. conventional activated sludge) impacts the optimum EBCT. Based on a comparison with the literature, the MBR filtrate in this study seemed to be highly recalcitrant with respect to oxidation and biodegradation. It is unclear whether this was a site-specific finding or if it is related to the efficacy of the MBR treatment process.
- Another key finding derived from the kinetics tests was the resilience in bulk biological activity to changes in the EBCT based on TOC removal after a stable biological community is developed. A time interval equivalent to three hydraulic retention times was sufficient for biological activity stabilization in the biofilters. However, this study did not fully address the development of micro-communities within the biofilters, which might be capable of specific treatment objectives (e.g., biodegradation of N-nitrosodimethylamine (NDMA), denitrification, bromate reduction). These micro-communities might be sensitive to rapid changes in EBCT.
- The highest ozone dose of 1.12 O<sub>3</sub>/TOC achieved the greatest reductions in bulk organic matter due to oxidation and subsequent biofiltration. At this ozone dose, reductions of up to 95% of fluorophores associated with soluble microbial products (region I), 92% of fluorophores associated with fulvic-like acids (region II), and 92% of fluorophores associated with humic-like substances (region III) were achieved. At this ozone dose and the optimum EBCT, the minimum TOC concentration attained was 5.0 mg/L. It is assumed that higher ozone doses would achieve even better water quality, but the data suggest that there is a point of diminishing return for ozone dosing as well.

- Some trace organic contaminants (e.g., the artificial sweetener acesulfame-K) actually increased during biofiltration, and 21 of the 103 target compounds were still detected after ozone-biofiltration. However, the literature suggests that the vast majority of these compounds pose no threat to public health at these low concentrations. The one exception is NDMA (12 ng/L in the ozone-anthracite effluent), which would necessitate further treatment to achieve the 10-ng/L regulatory threshold in California.
- Despite optimization, ozone-biofiltration systems alone appear to be insufficient to meet the stringent TOC target of 0.5 mg/L specified in California's potable reuse regulations. If higher ozone doses are used, this goal may be more attainable, but the current study suggests that TOC removal will plateau far before reaching a 0.5-mg/L effluent TOC concentration. Therefore, additional treatment steps would be necessary to achieve significantly lower concentrations of bulk organic matter. Possible strategies to comply with existing potable reuse regulations include increasing the percentage of diluent water or adding additional treatment steps. The 0.5 mg/L target in California applies to 100% recycled water. If diluent water is added, this target value will increase accordingly. Additional treatment options include a supplementary GAC column (with adsorption capacity) or an ion exchange resin suitable for TOC removal. Humbert et al. (2005) demonstrated 80% DOC removal with a 30-minute contact time using strong anion exchange resins, and GAC columns operated at 13 minute EBCTs achieved 65% TOC removal and over 70% DOC removal (Gibert et al., 2013). However, it is important to note that not all states have such stringent regulations on effluent TOC concentrations, and it is currently unclear whether such requirements have any direct link to public health. It is important to note that ozone-biofiltration is unable to reduce total dissolved solids (TDS) concentrations, which are typically high in wastewater. Therefore, additional treatment for TDS may also be needed in potable reuse applications.

## 5.0 Future Work

This study demonstrated the potential synergisms of ozone and biofiltration, but additional research must be conducted to validate and/or expand on some of the significant findings. The apparent logarithmic relationship that exists between  $O_3/TOC$  and EBCT was not fully established. Higher ozone doses must be explored and larger data sets gathered to better understand the relationship that may exist. Also of interest would be examining this relationship based on various water matrices and media type. If different water qualities yield similar results, correlations could be made and utilized by water utilities at any location. This would save time and money on ozone dosing and biofilter performance experiments.

Another possible avenue for research would be to analyze the effect of ozonated water on biofilm attachment to media and the composition of the microbial community. Conditions within biofiltration systems, particularly related to micro-communities, are largely unknown and must be evaluated to better understand how to optimize this type of water treatment. The

increasing understanding and use of metagenomics and proteomics may aid in this research endeavor.

Based on the performance of the biocatalyst in removing TOC, it would be worth investigating different column configurations and operational conditions to enhance the intended use of this media. For instance, an upflow biofilter (i.e., a fluidized bed) may be more suited for the biocatalyst since it was not designed for packed-bed applications. This would alleviate the issue of compaction and caking if fluidization could be achieved. The presence of dissolved oxygen likely inhibited denitrification; operating the biocatalyst in series with a BAC filter or using nitrogen gas for sparging may help alleviate this problem.

Finally, it is unclear what possible health effects are associated with bulk organic matter in ozone-biofiltration effluent. Therefore, the 0.5-mg/L TOC threshold may not be necessary to maintain public safety in potable reuse applications. Further examination of this bulk parameter is needed.

## **6.0 Information Transfer Activities**

1. Selvy, A., D. Gerrity. 2014. Optimization of Ozone-Biological Activated Carbon Treatment for Potable Reuse Applications. Nevada Water Resources Association 2014 Annual Conference, Las Vegas, NV, Jan. 2014. (2<sup>nd</sup> Place in Student Poster Contest) (see Appendix 2)
2. Selvy, A., D. Gerrity. 2015. Impacts Of Ozone Dose And Empty Bed Contact Time On Total Organic Carbon Removal Through Ozone-Biological Activated Carbon Treatment. 19<sup>th</sup> Annual Water Reuse and Desalination Research Conference, Huntington Beach, CA, May 2015. (see Appendix 3)

## **7.0 Student Support**

This grant largely funded the research endeavors (time, instruments, and travel) during completion of Ashley Selvy's M.S.E. degree, which was completed in May 2015. During her studies, Ashley presented a poster at the Nevada Water Resources Association's 2014 Annual Conference and was awarded 2<sup>nd</sup> Place in the student poster competition. Ashley also presented a poster at the 19<sup>th</sup> Annual Water Reuse and Desalination Research Conference. She intends to compile the information from this study in a manuscript that will be submitted to a peer-reviewed water/environmental engineering journal.

During the project, Dr. Gerrity also advised a team of senior design students who designed a hypothetical potable reuse treatment facility employing advanced oxidation and biological activated carbon for Searchlight, Nevada.

Dr. Gerrity also leveraged the information gathered during this study and the existing pilot

infrastructure to obtain additional external funding from the U.S. Environmental Protection Agency's STAR program: Early Career Awards – Human and Ecological Health Impacts Associated with Water Reuse and Conservation Practices (EPA-G2014-STAR-F2). The three-year EPA project is expected to start in August 2015 and will support at least two graduate students and several undergraduate students.

## 8.0 References

1. CDPH. (2014). Regulations related to recycled water. California Department of Public Health. Division of Drinking Water.  
[http://www.waterboards.ca.gov/drinking\\_water/certlic/drinkingwater/documents/lawbook/RWregulations\\_20140618.pdf](http://www.waterboards.ca.gov/drinking_water/certlic/drinkingwater/documents/lawbook/RWregulations_20140618.pdf). Accessed: May 14, 2015.
2. Gerrity, D., Gamage, S., Holady, J.C., Mawhinney, D.B., Quinones, O., Trenholm, R.A. and Snyder, S.A. (2011). Pilot-scale evaluation of ozone and biological activated carbon for trace organic contaminant mitigation and disinfection. *Water Research*, 45, 2155-2165.
3. Gerrity, D., Gamage, S., Jones, D., Korshin, G., Lee, Y., Pisarenko, A., . . . Snyder, S. (2012). Development of surrogate correlation models to predict trace organic contaminant oxidation and microbial inactivation during ozonation. *Water Research*, 46(19), 6257-6272.
4. Gerrity, D., Pecson, B., Trussell, R.S., Trussell, R.R. (2013) Potable reuse treatment trains throughout the world. *Journal of Water Supply: Research and Technology*, 62, 321-338.
5. Gerrity, D., Owens-Bennett, E., Venezia, T., Stanford, B.D., Plumlee, M.H., Debroux, J., Trussell, R.S. (2014). Applicability of ozone and biological activated carbon for potable reuse. *Ozone Sci. Eng.*, 36, 123-127.
6. Gerrity, D., Pisarenko, A.N., Marti, E., Trenholm, R.A., Geringer, F., Reungoat, J., Dickenson, E. (2015). Nitrosamines in pilot-scale and full-scale wastewater treatment plants with ozonation. *Water Research*, 72, 251-261.
7. Gibert, O., Benoit, L., Fernandez, M., Bernat, X., Paraira, M., & Pons, M. (2013). Fractionation and removal of dissolved organic carbon in a full-scale granular activated carbon filter used for drinking water production. *Water Research*, 47, 2821.
8. Horiba Scientific. (2012). Aqualog software user's guide for version 3.6 (Version 3.6 rev. B ed.). HORIBA Scientific.
9. Humbert, H., Gallard, H., Suty, H., & Croue, J. P. (2005). Performance of selected anion exchange resins for the treatment of a high DOC content surface water. *Water Research*, 39(9), 1699-1708.
10. IDEXX Laboratories. (2015). How colilert-18 works. Retrieved from <https://www.idexx.com/water/products/colilert-18.html>
11. Liu, J., Zhang, X., & Wang, Z. (2006). Nitrification and denitrification in BACF for treating high ammonia source water. *Huan Jing Ke Xue*, 27(1), 69-73.
12. Magic-Knezev, A., & van der Kooij, D. (2004). Optimisation and significance of ATP analysis for measuring active biomass in granular activated carbon filters used in water treatment. *Water Research*, 38, 3971-3979.
13. NWRI. (2013). Examining the criteria for direct potable reuse. National Water Research Institute. WateReuse Research Foundation. Alexandria, VA.

14. Pharand, L., Van Dyke, M., Anderson, W., & Huck, P. (2014). Assessment of biomass in drinking water biofilters by adenosine triphosphate. *Journal American Water Works Association*, 106(10), 63-64.
15. Rakness, K., Wert, E., Elovitz, M., & Mahoney, S. (2010). Operator-friendly technique and quality control considerations for indigo colorimetric measurement of ozone residual. *Ozone-Science & Engineering*, 32(1), 33-42.
16. Reungoat, J., Escher, B.I., Macova, M., Argaud, F.X., Gernjak, J.K. and Keller, J. (2012). Ozonation and biological activated carbon filtration of wastewater treatment plant effluents. *Water Research* 46, 863-872.
17. Reungoat, J., Macova, M., Escher, B.I., Carswell, S., Mueller, J.F. and Keller, J. (2010). Removal of micropollutants and reduction of biological activity in a full scale reclamation plant using ozonation and activated carbon filtration. *Water Research* 44, 625-637.
18. Sison, N., Hanaki, K., & Matsuo, T. (1995). High loading denitrification by biological activated carbon process. *Water Research*, 29(12), 2776-2779.
19. Sison, N., Hanaki, K., & Matsuo, T. (1996). Denitrification with external carbon source utilizing adsorption and desorption capability of activated carbon. *Water Research*, 30(1), 217-227.
20. Staehelin, J., & Hoigne, J. (1982). Decomposition of ozone in water: Rate of initiation by hydroxide ions and hydrogen peroxide. *Environmental Science and Technology*, 16(10), 676.
21. Velten, S. (2011). Development of biomass in a drinking water granular active carbon (GAC) filter. *Water Research*, 45, 6347-6354.
22. Velten, S. (2007). Rapid and direct estimation of active biomass on granular activated carbon through adenosine tri-phosphate (ATP) determination. *Water Research*, 41, 1973-1983.
23. Zhou, J. (2013). Improved fluorescence excitation-emission matrix regional integration to quantify spectra for fluorescent dissolved organic matter. *Journal of Environmental Quality*, 42, 925.

## Appendix 1. Fluorescence standard operating procedure.

\*Samples should be at room temperature, filtered (0.7  $\mu\text{m}$ ), and analyzed within 48 hours\*

1. Turn on computer and Aqualog instrument
2. Allow Aqualog to warm up for 15 minutes
3. Open Aqualog software
4. Raman measurement (perform 3 separate times each time the Aqualog is turned on)
  - a. Fill sample cell with nanopure water and place into holder
  - b. Click **H2O** button to initialize instrument and open 'Aqualog Main Experiment Menu'
  - c. Click **Spectra**
  - d. Click **Emission 2D**
  - e. Load archived experimental settings file or create new protocol
    - i. Use a consistent filing system so that you can recall old settings
  - f. Verify settings:
    - i. Change Data Identifier (used to identify sample in workgroup)
    - ii. Integration = 3 s
    - iii. Accumulations = 1
    - iv. Excitation Wavelength Park = 350 nm
    - v. Emission Wavelength Increment = 0.82 nm (2 pixel)
    - vi. CCD Gain = Medium
    - vii. Blank/Sample Setup = Sample Only
  - g. Click **Run**
  - h. (**Only on first run of workgroup**) Choose directory to save project file
    - i. Use a consistent filing system so that you can recall old files
    - ii. Only run 5-10 samples per project file (workgroup) to limit file size
  - i. Click **Emission Sample Data** tab
    - i. Click **File**  $\rightarrow$  **Export**  $\rightarrow$  **ASCII** and save file as a **.txt file** with tab separator
  - j. Open Excel and then open the exported file and save as an Excel Workbook
5. Sample Measurement
  - a. Fill one sample cell with nanopure water (to be used for blank)
  - b. Fill second sample cell with sample to be analyzed
  - c. Click **H2O** button to initialize instrument and open 'Aqualog Main Experiment Menu'
  - d. Click **3D**
  - e. Click **EEM 3D CCD + Absorbance**
  - f. Load archived experimental settings file or create new protocol
    - i. Use a consistent filing system so that you can recall old settings
  - g. Verify settings:
    - i. Change Data Identifier (used to identify sample in workgroup)
    - ii. Integration = 3 s
    - iii. Excitation Range: High = 470 nm, Low = 240, Increment = 1 nm
    - iv. Emission Wavelength Increment = 0.82 nm (2 pixel)
    - v. CCD Gain = Medium

- vi. Blank/Sample Setup = Sample and Blank
  - 1. Collect blank on first run or load archived blank from that day
- h. Click **Run**
- i. **(Only on first run of workgroup)** Choose directory to save project file
  - i. Use a consistent filing system so that you can recall old files
  - ii. Only run 5-10 samples per project file (workgroup) to limit file size
- j. Click **Abs Spectrum Sample** tab
  - i. Click **File → Export → ASCII** and save file as a **.txt file** with tab separator
- k. Click **Sample – Blank Waterfall Plot** tab
  - i. Click **Inner Filter Effect** button (next to H<sub>2</sub>O)
- l. Click **Processed Graph: IFE** tab
  - i. Click **Rayleigh Masking** button (next to IFE)
  - ii. “Mask 1<sup>st</sup> Order Rayleigh” should be checked
  - iii. “Mask 2<sup>nd</sup> Order Rayleigh” should be checked
  - iv. “SUM of slit widths (in bandpass)” should be 10
- m. Click **Processed Data: IFE\_RM** tab
  - i. Click **File → Export → ASCII** and save file as a **.txt file** with tab separator
- n. Save all files in a permanent folder named according to sample description
- 6. Process the data with MATLAB
  - a. Open Excel and then open the **Processed Data: IFE\_RM** file and save as an Excel Workbook
  - b. Open the **Abs Spectrum Sample** file and save as an Excel Workbook
  - c. Move a copy of the following files to your “working” folder for MATLAB analysis
    - i. The 3 **Raman** Excel files
    - ii. The **Processed Data: IFE\_RM** Excel file
    - iii. The **Abs Spectrum Sample** Excel file
    - iv. Verify that your “working” folder also contains the **ABS and FRI** Excel files
  - d. Open the appropriate MATLAB code (Aqualog.m)
  - e. Verify that the MATLAB home screen is linked to your working folder.
  - f. Verify that all directories in the MATLAB code (purple text) are valid.
  - g. Run the program.
  - h. Move all processed data to permanent folder. Only move a copy of the **FRI** and **ABS** Excel files to your permanent folder. These files must remain in your working folder for future processing.





# Impacts of Ozone Dose and Empty Bed Contact Time on Total Organic Carbon Removal Through Ozone-Biological Activated Carbon Treatment

Ashley Selvy, B.S.C.E., E.I.T., Daniel Gerrity, Ph.D., Assistant Professor  
Department of Civil and Environmental Engineering and Construction, University of Nevada, Las Vegas



## INTRODUCTION

In the face of global climate change, water scarcity has become a global threat. These conditions have created "pristine" drinking water sources.

There is considerable debate as to the level of treatment needed to ensure protection of public health with regard to possible reuse. Among existing potable reuse guidelines and regulations, the California Division of Water Resources (CDWR) has set a standard for water quality. For example, wastewater-derived total organic carbon (TOC) is limited to 0.5 mg/L for direct injection of non-diluted reuse water into any California aquifer. Currently, the only way to meet these standards is through the use of full advanced oxidation process (AOP), which consists of reverse osmosis (RO) and an advanced oxidation process (AOP). While RO is highly effective at treating water for reuse, it is difficult to maintain, and AOPs are costly.

Alternative treatment trains composed of ozone and biological activated carbon (BAC) have been employed in several locations throughout the world, but these systems have not yet been optimized and are unable to compete with RO-based treatment trains on the basis of TOC removal.

With the exception of TOC and total dissolved solids (TDS), which are generally more relevant to aesthetics rather than public health, ozone-BAC is a promising alternative to RO-based treatment trains. Ozone-BAC treatment trains on the basis of pathogen reduction, trace organic contaminant (TOC) mitigation, and a variety of other parameters (Reungoak et al., 2010, 2012; Gerrity et al., 2011, 2014). There are also significant energy and cost savings for the ozone-BAC alternative as there is an incentive to investigate various operational configurations for ozone-BAC treatment trains to achieve greater TOC removal (Gerrity et al., 2014; Sappier et al., 2014).



Figure 1. Photo of the (A) ozone contactors and fill grids systems schematic. The pink asterisks mark the baffler effluent sampling locations, the white 'X's represent the lower media sampling and effluent sample locations. The influent sample port was located prior to ozone injection into the water stream, and the effluent sample location was located after the ozone contactors. The column containing the biocatalyst is denoted as BC. Photo of the (B) BAC columns (columns BC is not shown).



Figure 2. Schematic diagram of the reactor effluent and sampling locations. The white 'X's represent the lower media sampling and effluent sample locations. The influent sample port was located prior to ozone injection into the water stream, and the effluent sample location was located after the ozone contactors. The column containing the biocatalyst is denoted as BC. Photo of the (C) BAC columns (columns BC is not shown).

## OZONE DEMAND/DECAY

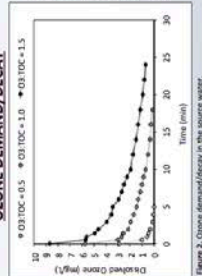


Figure 3. Ozone demand/decay in this source water.

## OZONE DOSING

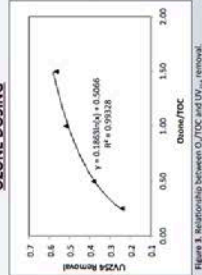


Figure 4. Relationship between O<sub>3</sub>:TOC and UV<sub>254</sub> removal.

## KINETICS TESTS

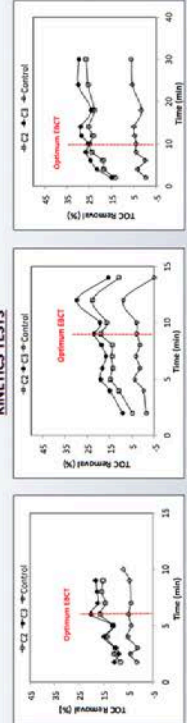


Figure 5. TOC removal with O<sub>3</sub>:TOC=0.82 at various EBCTs.

## KINETICS TEST RESULTS SUMMARY

The data from Table 1 was used to develop a relationship between optimum EBCT and ozone dose. The relationship function appears to capture the relationship well, but additional data are warranted to further validate the relationship. The relationship of ATP indicator of bacteria and the degree of biological growth in a system.

O <sub>3</sub> :TOC	Optimum EBCT (min)	Minimum TOC Removal (%)	Minimum TOC (mg/L)	Minimum ATP (mg/L)
0.35	6	15	20	6.4
0.62	9	19	22	5.7
1.12	10	25	23	3.0

## BIOFILM CHARACTERIZATION

EBCT (min)	ATP (mg/L)	ATP (mg/L)	ATP (mg/L)
C1	8.1457E+06	3.2420E+06	1.8770E+06
C2	9.1457E+06	2.2420E+06	1.8770E+06
Control	N/A	2.0457E+06	N/A
BC	2.3457E+06	1.8770E+06	N/A

## CONCLUSIONS

- The optimum EBCT for O<sub>3</sub>:TOC of 0.35, 0.62, and 1.12 were found to be 6, 9, and 10 minutes, respectively. The relationship between O<sub>3</sub>:TOC and biological EBCTs appears to exist between the two parameters. Based on this relationship, it appears that relatively low EBCTs are necessary for TOC removal in some matrices; however, additional testing is warranted to validate the relationship.
- The small media provided more surface area for biological growth, which explains the higher ATP concentration found on the small media. The small media also provided more surface area for TOC removal and the small media, although improved hydraulic performance may also contribute.
- At the highest O<sub>3</sub>:TOC ratio of 1.12 and EBCT of 10 minutes, the minimum TOC concentration attained was 5.0 mg/L. It is assumed that higher ozone doses would achieve even better water quality, but the data suggest that there is a point of diminishing return for ozone dosing as well.
- Despite epidemiologic, O<sub>3</sub>:BAC systems, alone are insufficient to meet the California Division of Water Resources (CDWR) TOC of 0.5 mg/L. If higher ozone doses were used, this goal may have been more attainable, but the data suggests the TOC removal would plateau far before reaching a 0.5 mg/L effluent TOC concentration.
- Possible strategies to comply with existing potable reuse regulations include increasing the percentage of diluent water or adding additional treatment steps, such as ion exchange or activated carbon with adsorptive capacity.

## FUTURE WORK

- The apparent logarithmic relationship that exists between O<sub>3</sub>:TOC and EBCT was not fully established. Higher ozone doses must be explored and the data sets gathered to better understand the relationship that may exist.
- Analyze the effect of coagulated water on biofilm attachment to media and biological community makeup.
- It is unclear what possible health effects are associated with TOC; therefore, the 0.5 mg/L threshold may not be necessary to maintain public safety in potable reuse applications. Further examination of this risk parameter is needed.

## REFERENCES

- Gerrity, D., Gamage, S., Holsby, J.C., Mawhinney, D.B., Quinones, O., Tresham, R.A., and Snyder, S.A. (2011) Pilot-scale evaluation of ozone and biological activated carbon for trace organic contaminant mitigation and disinfection. Water Research 45, 2153-2163.
- Gerrity, D., Owens-Bennett, E., Hernandez, T., Stanbury, B.D., Purnelle, J., and Snyder, S.A. (2012) Ozone-Biological Activated Carbon: Biological Activated Carbon for Potable Reuse. Ozone 5(1), Eng. 35, 123-137.
- Reungoak, J., Escher, B., Macova, M., Arnaud, F.X., Gerrity, J.K. and Keller, J. (2012) Oxidation and biological activated carbon filtration of wastewater treatment plant effluents. Water Research 46, 863-872.
- Reungoak, J., Meehan, M., Escher, B.L., Corwell, S., Mueller, J.F., and Keller, J. (2010) Removal of micropollutants and reduction of biological carbon filtration. Water Research 44, 625-637.
- Snyder, S.A., von Gunten, U., Amy, G. and Debroux, J. (2014) Use of ozone in water reclamation for contaminant oxidation. WRF-08-05. Water Reuse Research Foundation.

## ACKNOWLEDGEMENTS

I would like to thank Dr. Daniel Gerrity for providing me with the opportunity to pursue this research. I would also like to thank staff at the study site for providing not only a continuous supply of water but the space to perform the research. The project grant was funded by the publication of Grant Ecological Survey. Its contents are solely the responsibility of the authors and do not necessarily represent the official views of the USGS.

## SYSTEM DESCRIPTION

Membrane bioreactor (MBR) filtrate fed the 0.5 lpm pilot system (Figure 1). An ozone generator and injection into the feed water. The ozone contactors ranged from 1-2 inches in diameter and provided a total of approximately 25 minutes of contact time. Exhausted 1.2 mm Calgon carbon was loaded into parallel 1-inch columns (C1, C2, C3) receiving coagulated MBR filtrate and a C3 column of exhausted 0.05 calgon carbon and BAC media. The BAC media was biocatalyst (polyvinyl alcohol bead containing denitrifying microorganisms).

## BIOFILTER EVALUATION

The ozone-BAC pilot was operated long term for biofilm stabilization and TOC removal. The system was operated for 11 months after start-up. The system was re-evaluated to determine the cause of the unexpected results. Two theories were tested:

- If the media to column diameter ratio is too large, hydraulic inefficiencies due to wall effects may occur. To test this theory, C3 was replaced with a smaller media of 0.35 mm 11 months after start-up.
- It was theorized that the bioavailable TOC was being consumed quicker than the TOC was being added. To test this theory, the system was replaced with a smaller media of 0.35 mm 11 months after start-up.

EBCT would have little impact on bulk biological activity. To study these theories, kinetics tests with shorter EBCTs were performed. Three kinetics tests were performed for this study. Each one was targeting a different O<sub>3</sub>:TOC ratio. It should be noted that the only samples collected during the kinetics tests were influent, C1, control, and effluent. C1 and C3 were redundant given that they contained the same media as C2. Due to severe compaction of the polyvinyl alcohol biofilms, the flow rates were extremely low and could not be adjusted to flow rates necessary for the tests.

# Estimation of Atmospheric Wet and Dry Deposition of Nutrients to Lake Tahoe Snowpack

## Basic Information

<b>Title:</b>	Estimation of Atmospheric Wet and Dry Deposition of Nutrients to Lake Tahoe Snowpack
<b>Project Number:</b>	2013NV195B
<b>Start Date:</b>	3/1/2013
<b>End Date:</b>	2/28/2015
<b>Funding Source:</b>	104B
<b>Congressional District:</b>	NV002
<b>Research Category:</b>	Water Quality
<b>Focus Category:</b>	Nutrients, Hydrology, Water Quality
<b>Descriptors:</b>	None
<b>Principal Investigators:</b>	Rina Schumer

## Publications

- Obrist, D., Moore, C. W., Pearson, C., Pierce, A. M., Schumer, R., Helmig, D., Van Dam, B., Fain, X., Steffen, A., Staebler, R., Nghiem, S., Douglas, T., 2013: Mercury in alpine and Arctic snow: atmospheric deposition and fate processes, Seminar, Graduate Program of Hydrologic Sciences, University of Nevada: Reno, NV, April 1, 2013
- Pearson, C., Obrist, D., Schumer, R., 2013: Nutrient and Mercury Concentrations and Loads in Tahoe Basin Snowpack, AGU Fall Meeting: San Francisco, CA, December 9, 2013
- Pearson, C., Obrist, D., Schumer, R., 2013: Nitrogen and Phosphorus Concentrations and Loads within Lake Tahoe Snowpack, University Council on Water Resources 2013 Annual Conference: Lake Tahoe, CA, June 1, 2013, Published
- Obrist, D., Moore, C. W., Douglas, T. A., Steffen, A., Staebler, R. M., Pearson, C., 2012: Concentrations of total and dissolved Hg in snow and vapor deposition collected during Atmospheric Mercury Depletion Events (AMDEs) in Barrow, Alaska during the BROMEX campaign. Abstract A31D-0059, AGU Fall Meeting: San Francisco, CA
- Pearson, C., Obrist, D., Schumer, R., 2012: Quantifying Nutrient and Mercury Concentrations and Loads in Tahoe Snowpack, Water Summit 2012: Milwaukee, WI.
- Pearson, C., Obrist, D., Schumer, R., 2012: Quantifying Nutrient and Mercury Concentrations and Loads in Lake Tahoe Snowpack, Abstract B23H-0540, Presentation at AGU 2012 Fall Meeting: San Francisco, CA, December 3, 2012.
- Trustman, B. D., Obrist, D., Schumer, R., Pearson, C., Moore, C. W., 2014: Nutrient and Mercury Dynamics in the Lake Tahoe basin Snowpack, Mountain Observatories: Reno, NV, July 18, 2014
- Pearson, C., Schumer, R., Trustman, B. D., Rittger, K., Johnson, D. W., Obrist, D. (2015). Nutrient and mercury deposition and storage in an alpine snowpack of the Sierra Nevada, USA, Biogeosciences Discuss., 12, 593-636

**2015 NIWR Project 2013NV195B Update and Final Report  
Estimation of atmospheric wet and dry deposition of nutrients  
to Lake Tahoe Snowpack**

**Rina Schumer, Division of Hydrologic Sciences, Desert Research Institute  
Daniel Obrist, Division of Atmospheric Sciences, Desert Research Institute**

### **Problem and Research Objectives**

This study aims to fill gaps in nitrogen, phosphorous, and mercury deposition loads contained in snowfall and snowpack throughout the Tahoe basin using experimental measurements and spatial modeling. Developing atmospheric deposition constraints is needed to understand mobility and transport pathways of N and P from the watersheds to the lake, which account for a significant fraction of nutrient inputs to the lake. Comprehensive management practices to reduce N and P loads to Lake Tahoe will benefit from improved estimates of nutrient deposition to terrestrial basin areas, particularly since these provide a long-term source for potential N and P inputs to Lake Tahoe. Measurement and modelling of mercury deposition was added to this project in an effort to extend expertise in Mercury cycling in high alpine watersheds.

We will fill the gap in Tahoe Basin terrestrial atmospheric deposition estimates using an integrated approach that includes experimental measurements of wet deposition loads and snowpack accumulation in the Lake Tahoe watershed, combined with spatial modeling to extrapolate snowpack loads of N, P, and Hg to the entire watershed area. The role of snowpack deposition of nutrients is considered key in the Lake Tahoe basin given that seventy percent of annual precipitation occurs during winter and spring as snow and results from a National Atmospheric Deposition Program (NADP) stations in Sagehen Creek indicating that up to two-thirds of annual wet deposition of nutrients is associated with winter and spring snowfall.

### **Methods**

Wet deposition loads in the basin are measured using both wet deposition samplers and snowpack core sampling. A number of wet deposition samplers are deployed in the Lake Tahoe watershed to continuously collect wet deposition samples, one located at a high elevation, remote site on top of Homewood ski area and a second location in Incline Village, NV. Since the Lake Tahoe Basin straddles the boundary of Nevada and California, field work will occur in both states. Wet deposition samples are collected every two weeks. Along with bi-weekly wet deposition samples, snowpack core samples will be collected at seven sites in the basin, starting with the first measureable snowpack accumulation until spring melting has ended. These sites are distributed across elevations and along eastern and western transects, with three sites located in the western part of the watershed in California and four sites in Nevada

Basin-wide loads and distribution are assessed using chemical concentrations and loads measured throughout the snow seasons as well as basin-wide mean peak SWE estimates from SWE reconstruction for the Sierra Nevada from 2000 to 2011. Sierra SWE reconstruction employs accurate estimates of snow depletion rates based on MODIS Snow Covered Area and Grain size (MODSCAG) in order to estimate peak SWE. MODSCAG calculates fractional snow cover area and grain size from Moderate Resolution Imaging Spectroradiometer (MODIS) data.

### **Principal findings and significance**

Bi-weekly snowpack core samples were collected at seven sites along two elevation gradients in the Tahoe Basin during two consecutive snow years to evaluate total wintertime snowpack accumulation of nutrients and pollutants in a high elevation watershed of the Sierra Nevada. Additional sampling of wet deposition and detailed snow pit profiles was conducted the following year to compare wet deposition to snowpack storage and assess the vertical dynamics of snowpack chemicals. Results show that on average organic N comprised 48% of all snowpack N, while nitrate ( $\text{NO}_3\text{-N}$ ) and TAN (total ammonia nitrogen) made up 25 and 27%, respectively. Snowpack  $\text{NO}_3\text{-N}$  concentrations were relatively uniform across sampling sites over the sampling seasons and showed little difference between seasonal wet deposition and integrated snow pit concentrations in agreement with previous studies that identify wet deposition as the dominant source of wintertime  $\text{NO}_3\text{-N}$  deposition. However, vertical snow pit profiles showed highly variable concentrations of  $\text{NO}_3\text{-N}$  within the snowpack indicative of additional deposition and in snowpack dynamics. Unlike  $\text{NO}_3\text{-N}$ , snowpack TAN doubled towards the end of winter and in addition to wet deposition, had a strong dry deposition component. Organic N concentrations in snowpack were highly variable (from 35 to 70%) and showed no clear temporal or spatial dependence throughout the season. Integrated snowpack organic N concentrations were up to 2.5 times higher than seasonal wet deposition, likely due to microbial immobilization of inorganic N as evident by coinciding increases of organic N and decreases of inorganic N, in deeper, aged snowpack. Spatial and temporal deposition patterns of snowpack P were consistent with particulate-bound dry deposition inputs and strong impacts from in-basin sources causing up to 6 times enrichment at urban locations compared to remote sites. Snowpack Hg showed little temporal variability and was dominated by particulate-bound forms (78% on average). Dissolved Hg concentrations were consistently lower in snowpack than in wet deposition which we attribute to photochemical-driven gaseous remission. In agreement with this pattern is a significant positive relationship between snowpack Hg and elevation, attributed to a combination of increased snow accumulation at higher elevations causing limited light penetration and lower photochemical re-emission losses in deeper, higher elevation snowpack. Finally, estimates of basin-wide loading based on spatially extrapolated concentrations and a satellite-based snow water equivalent reconstruction model identify snowpack chemical loading from atmospheric deposition as a substantial source of nutrients

and pollutants to the Lake Tahoe basin, accounting for 113 t of N, 9.3 t of P, and 1.2 kg of Hg each year.

## Information Transfer Activities

### Presentations

- Trustman, B. D., Obrist, D., Schumer, R., Pearson, C., Moore, C. W., 2014: Nutrient and Mercury Dynamics in the Lake Tahoe basin Snowpack, Mountain Observatories: Reno, NV, July 18, 2014
- Obrist, D., Moore, C. W., Pearson, C., Pierce, A. M., Schumer, R., Helmig, D., Van Dam, B., Fain, X., Steffen, A., Staebler, R., Nghiem, S., Douglas, T., 2013: Mercury in alpine and Arctic snow: atmospheric deposition and fate processes, Seminar, Graduate Program of Hydrologic Sciences, University of Nevada: Reno, NV, April 1, 2013
- Pearson, C., Obrist, D., Schumer, R., 2013: Nutrient and Mercury Concentrations and Loads in Tahoe Basin Snowpack, AGU Fall Meeting: San Francisco, CA, December 9, 2013
- Pearson, C., Obrist, D., Schumer, R., 2013: Nitrogen and Phosphorus Concentrations and Loads within Lake Tahoe Snowpack, University Council on Water Resources 2013 Annual Conference: Lake Tahoe, CA, June 1, 2013, Published
- Obrist, D., Moore, C. W., Douglas, T. A., Steffen, A., Staebler, R. M., Pearson, C., 2012: Concentrations of total and dissolved Hg in snow and vapor deposition collected during Atmospheric Mercury Depletion Events (AMDEs) in Barrow, Alaska during the BROMEX campaign. Abstract A31D-0059, AGU Fall Meeting: San Francisco, CA
- Pearson, C., Obrist, D., Schumer, R., 2012: Quantifying Nutrient and Mercury Concentrations and Loads in Tahoe Snowpack, Water Summit 2012: Milwaukee, WI,
- Pearson, C., Obrist, D., Schumer, R., 2012: Quantifying Nutrient and Mercury Concentrations and Loads in Lake Tahoe Snowpack, Abstract B23H-0540, Presentation at AGU 2012 Fall Meeting: San Francisco, CA, December 3, 2012,

### Publications

- Pearson, C., Schumer, R., Trustman, B. D., Rittger, K., Johnson, D. W., Obrist, D. (2015). Nutrient and mercury deposition and storage in an alpine snowpack of the Sierra Nevada, USA, *Biogeosciences Discuss.*, 12, 593-636

### Student Support

This project supported the Master's work for Chris Pearson, who graduated in December 2013 and partially supported Master's student Benjamin Trustman. The project produced numerous conference presentations (above) and a published manuscript with both students as coauthors in *Biogeosciences*.

# Quantifying Surface Runoff and Water Infiltration in Arid and Semi-arid Areas

## Basic Information

<b>Title:</b>	Quantifying Surface Runoff and Water Infiltration in Arid and Semi-arid Areas
<b>Project Number:</b>	2013NV196B
<b>Start Date:</b>	3/1/2013
<b>End Date:</b>	2/28/2016
<b>Funding Source:</b>	104B
<b>Congressional District:</b>	NV001
<b>Research Category:</b>	Climate and Hydrologic Processes
<b>Focus Category:</b>	Surface Water, Models, Water Quantity
<b>Descriptors:</b>	None
<b>Principal Investigators:</b>	Yong Zhang, Li Chen, Donald M Reeves

## Publications

1. Zhang, Y., L. Chen, D. M. Reeves, and H.G. Sun, Fractional-derivative models for surface runoff along heterogeneous ground surface. Abstract will be published in the 2014 International Conference on Fractional Differentiation and its Applications, Catania, 23-25 June, 2014.
2. Sun, H.G., M. M. Meerschaert, Y. Zhang, J.T. Zhu, and W. Chen, A fractal Richards' equation to capture the non-Boltzmann scaling of water transport in unsaturated media, *Advances in Water Resources*, 52, 292-295, 2013.
3. Sun, H.G., Y. Zhang, W. Chen, and D. M. Reeves, Use of a variable-index fractional-derivative model to capture transient dispersion in heterogeneous media, *Journal of Contaminant Hydrology*, 157, 47-58, 2014.
4. Chen, L., 2014: Modeling Rainfall Runoff Process and Scaling Effects in Complex Arid Environments, 1st Congress of China Geodesy and Geophysics: Beijing, October 25, 2014-October 26, 2014.
5. Chen, L., Sela, S., Svoray, T., Assouline, S., 2014: Hydrological responses and scaling effects in vegetated semi-arid areas with surface sealing, (Invited talk), AGU Fall Meeting: San Francisco, December 15, 2014-December 19, 2014.

# **Progress Report for Quantifying surface runoff and water infiltration in arid and semi-arid areas**

**Li Chen**

## **Problem and Research Objectives**

Surface runoff is a fundamental hydrologic component that can affect many processes in hydrology, morphology, biology, and ecology. In arid and semi-arid areas, surface runoff in the form of Horton overland flow is often observed, due to the typical short-duration and high-intensity rainfall that easily exceeds the soil infiltration capacity. It can cause environmental effects (i.e., nonpoint source pollution and water sustainability), agriculture issues (i.e., reduction of crop productivity due to soil conservation), and natural hazards (i.e., flooding). Surface runoff is also the main driving force for soil erosion and may trigger debris flow hazards. It also produces horizontal redistribution of water resources that may affect habitats and ecosystem in watersheds, and rapidly transport of nutrients or contaminants along land surfaces which affects multiple biological and ecological processes. Accurate quantification of surface runoff, however, has remained a challenge in hydrology for many decades. This project proposes the use of novel mathematical models to quantify the complex dynamics of surface runoff and infiltration in order to protect water resources and the environment in Nevada.

## **Methodology**

In this study, we applied state-of-the-art physical theories and novel mathematical tools to build and solve the physical models for the surface runoff process. Random walk theories combined with the subordination technique can account for the nonlocal movement of water packages along a ground surface exhibiting fractal complexity. The local variations of flow behavior can also be captured by conditioning on local soil and topography properties. The resultant model explains the scale evolution of surface runoff within and across sub-basins through the use of the new mathematical concept of tempered stable laws. We have also generalized the Richards' equation using the physical concept of fractal time, which accounts for both the sub-diffusive and super-diffusive anomalous motion of moisture observed in heterogeneous, unsaturated soils. Meanwhile, we developed a high resolution, multidimensional conceptual modeling approach to simulate infiltration and runoff at various scales to explore the scale dependence runoff generation processes.

## **Principal Findings and Significance**

To date, the following findings are obtained through this study:

1. The infiltration process can be efficiently captured by a fractal Richards' equation (FRE). The traditional Richards' equation corresponds to the Boltzmann scaling of wetting front, with travel distance growing as the square root of time. In laboratory experiments and field measurements, the evolution of a horizontal wetting front can deviate significantly from Boltzmann scaling. The proposed fractal Richards' equation is able to capture the non-Boltzmann scaling of water transport in unsaturated soils, which replaces the integer-order time derivative of water content with a fractal derivative. Applications show that the FRE fits well water content curves from various previous literature.

2. The multi-scale heterogeneity nature of soils, especially the soil fractal dimension, may result in a full range of anomalous dynamics in water infiltration. This includes the sub-diffusive regime, when regions of flow permeability can retard flow, and super-diffusion, where the wetting front is accelerated along preferential flow paths. The fractal time index in the FRE model may be related to soil texture parameters, especially the fractal dimension.

3. Surface runoff and water infiltration in arid and semi-arid areas may not exhibit constant scaling; instead transition between diffusive states (i.e., super-diffusion, sub-diffusion, and Fickian diffusion) may occur at various transport scales. These transitions are likely attributed to physical properties of the medium, such as spatial variations in heterogeneity in soil and topography. This "transient dispersion" can be modeled with a variable-index fractional-derivative law (FDL) which is not limited to stationary heterogeneous media as the standard constant-index FDL limited. Applications show that the variable-index theory can efficiently quantify the observed scale transitions, with the scale index varying linearly in time or space.

5. A fractional-order continuity equation can be used to quantify the behavior of surface runoff, where the influence of heterogeneity on flow dynamics can be characterized using spatiotemporally nonlocal terms built upon fractional derivatives. The model is found capable to describe the general patterns of hillslope runoff hydrograph. Numerical analysis show that the space-fractional diffusive term in the flow model does not lead to apparent early arrivals in the rising limb of a hydrograph. Meanwhile, the time-fractional term in the model can account for the strong time-nonlocal influence of net recharge on the receding limb of a hydrograph, and a wide range of late-time behavior of flow.

6. The high resolution modeling study shows that surface runoff has a decline trend with the increase of the spatial scale in complex arid environment comprising a number of impacting environmental factors such as soil, topography and vegetation. This trend can be described by a power-law runoff-scale relationship. Such a relationship, however, can be affected by soil hydraulic properties, rainfall pattern and intensity. Large spatial

heterogeneity may increase the scale effect, while higher rainfall intensity may reduce the effect. This trend can be potentially used to guide the upscaling strategies in larger scale hydrologic modeling practice.

### **Information Transfer Activities:**

#### Papers:

- Chen, L. Sela S. Assouline, S., Zhang, Y. Scaling of rainfall-runoff in complex semi-arid environments. *Water Resources Research* (submitted).
- Zhang, Y., L. Chen, D. M. Reeves, and H. G. Sun, A fractional-order tempered-stable continuity model to capture surface water runoff, *Journal of Vibration and Control*, 2014. doi: 10.1177/1077546314557554.
- Sun, H.G., M. M. Meerschaert, Y. Zhang, J.T. Zhu, and W. Chen, A fractal Richards' equation to capture the non-Boltzmann scaling of water transport in unsaturated media, *Advances in Water Resources*, 52, 292-295, 2013.
- Sun, H.G., Y. Zhang, W. Chen, and D. M. Reeves, Use of a variable-index fractional-derivative model to capture transient dispersion in heterogeneous media, *Journal of Contaminant Hydrology*, 157, 47-58, 2014.

#### Presentations:

- Chen, L., Sela, S., Svoray, T., Assouline, S., 2014: Hydrological responses and scaling effects in vegetated semi-arid areas with surface sealing, (Invited talk), AGU Fall Meeting: San Francisco, December 15, 2014-December 19, 2014.
- Chen, L., 2014: Modeling Rainfall Runoff Process and Scaling Effects in Complex Arid Environments, 1st Congress of China Geodesy and Geophysics: Beijing, October 25, 2014-October 26, 2014.
- Zhang, Y., L. Chen, D. M. Reeves, and H.G. Sun, Fractional-derivative models for surface runoff along heterogeneous ground surface. International Conference on Fractional Differentiation and its Applications, Catania, 23-25 June, 2014.

### **Student support**

This project provided partial support for the Ph.D. graduate student Nudthawud Homtong and postdoctoral fellow Peng Jiang.

# Impact of climate on mercury transport in the Carson River-Lahontan Reservoir system and Management Alternatives to Mitigate Response

## Basic Information

<b>Title:</b>	Impact of climate on mercury transport in the Carson River-Lahontan Reservoir system and Management Alternatives to Mitigate Response
<b>Project Number:</b>	2013NV197B
<b>Start Date:</b>	3/1/2013
<b>End Date:</b>	6/30/2015
<b>Funding Source:</b>	104B
<b>Congressional District:</b>	NV002
<b>Research Category:</b>	Water Quality
<b>Focus Category:</b>	Non Point Pollution, Surface Water, Models
<b>Descriptors:</b>	None
<b>Principal Investigators:</b>	Rosemary Woods-Hart Carroll

## Publications

1. Flickinger, A. K., Carroll, R. W., Warwick, J. J., Schumer, R. (2015). Impact of Climate Change on Mercury Transport along the Carson River-Lahontan Reservoir System, Nevada Water Resources Association: Reno, NV, January 26, 2015.
2. Flickinger, A. K., Carroll, R. W., Warwick, J. J., Schumer, R. (2014). Impact of climate change on mercury transport along the Carson River-Lahontan Reservoir system, American Geophysical Union: San Francisco, CA, December 15, 2014-December 19, 2014, H31H-0734.

## Impact of climate on mercury transport in the Carson River-Lahontan Reservoir system

### Problem and Research Objective

The United States Environmental Protection Agency (US EPA) designated the Carson River and Lahontan Reservoir (CRLR) as a superfund site in 1991 for its contamination by mercury (Hg) as a result of historic mining practices. Fish populations in Lahontan Reservoir exceed the Federal Action limit for consumption (1 µg/g). The rate of Hg transported through the CRLR system and the resulting bioaccumulation in the reservoir is non-linearly related to in-stream flow (Carroll et al., 2000; Carroll et al., 2001; Carroll et al., 2004; Warwick and Carroll, 2008; Carroll, 2010). It is therefore vitally important to relate changes to in-stream flow regimes caused by climate change with the fate of Hg in this important freshwater system. Studies (IPCC, 2007; USGCRP, 2009) suggest that the future envelopes of climate variability may differ from historical data, with all regions in the southwestern US predicted to have increased temperatures and most regions predicted to experience a change in precipitation. The US Bureau of Reclamation (USBR, 2011) developed hydrologic responses associated with 112 down-scaled climate projections from the World Climate Research Programme Coupled Model Inter-comparison Project 3. Hydrologic projections are based on the Variable Infiltration Capacity (VIC) macro-scale hydrology model. The projected flows at Fort Churchill on the Carson River show that while uncertainty in projected flows increases significantly by 2070s, there is also significant increase in the median seasonal flow volume in the winter and a decrease in flows during the spring-summer runoff period. This change in precipitation will lead to changes in stream flow, which could affect the Hg transport in the CRLR system. This project aims to establish the impact of projected climate on Hg transport through the CRLR system and the significance of change in terms of timing and total mass of each Hg species modeled (total Hg, total dissolved Hg, total methylmercury (MeHg) and total dissolved MeHg).

### Methodology

#### Data Preparation

1. Observed flows at the Woodfords gage (10310000) on West Carson, Gardnerville gage (10309000) on the East Carson were correlated to predict historic flows at the Carson City Gage (gage number 10311000) on the main Carson River, from 1990 to present. This transfer is necessary since the CRLR Hg transport model uses the Carson City gage as its upstream flow boundary, not the Woodville or Gardnerville gages predicted by VIC. Data were separated by month and log-log regressions were performed to correlate the data. September and October were split in half to improve correlation and was likely required based on late season irrigation practices.
2. The bias correction process from “West-Wide Climate Risk Assessments: Bias-Corrected and Spatially Downscaled Surface Water Projections” was followed to reduce the existing bias between the observed and VIC predicted flows in the historical period. To do this, an empirical cumulative distribution function (ECDF) was found for both the observed and the projected data from 1950-1999. The VIC predicted output was then transformed by finding the percentile of the flow according to the ECDF of the projected data, and then using that percentile to find the corresponding flow in the ECDF of the observed data, which was used as the bias corrected flow and performed for Woodfords, Gardnerville and Fort Churchill Gages (10312000). Error in VIC bias-corrected flows reduced error (nrmse) from greater than 14% at all gage locations to 3.4% at Woodfords, 3.6% at Gardnerville and 4.1% at Fort Churchill for the historic record 1950-1999.
3. Bias correction factors calibrated for the historic record were applied to future VIC predictions for years 2000 to 2099. Future Woodville and Gardnerville flows were then translated into

Carson City Gage flows based on regression statistics described in (1). Carson City gage and Fort Churchill gage daily flows were used to develop RIVMOD input.

4. The Hg transport model requires the stage of the Lahontan Reservoir and the discharge from the Lahontan Dam as inputs. A spreadsheet model was created to model these parameters from the available data. The inputs to the spreadsheet are the average monthly flow from the Fort Churchill gage, representing the input from the Carson River, and the Truckee Canal (which enters the Lahontan Reservoir near the dam on the northern end of the reservoir). The initial storage, found from USGS gage data (10312100), is also set. Stage is then tracked as a function of inputs as well as the required release due to agricultural demands downstream and maximum reservoir stage.
5. The calibrated reservoir model was run over future VIC scenarios from 2000 to 2099 using average monthly Truckee Canal inflows to establish future reservoir stages and discharged based on historic reservoir operations. Reservoir discharge and stage, along with Truckee Canal inflows were input to RIVMOD at the daily stress period for future WASP/RIVMOD simulations.

### Model Modifications

Several modifications were made to the Hg Transport model in order to ensure that the runs could accurately run for a century. The original model had not been run for longer than a decade, and early attempts to continue the model past a decade found that the time variables needed to have more significant digits in order to prevent round off error. There was also a numerical instability that was solved by limiting the maximum change in Hg concentration between time steps, and the accuracy of the results was improved by raising the maximum number of iterations per time step from 10 to 20.

### Analysis:

Analysis was done for all 112 climate projections with respect to each modeled Hg species and total mass transported at the FCH as well as each of the three reservoir basins. Decadal daily-averages were determined as well as the 80% confidence interval based on ranking. Changes in decadal means were tested using the two-sample Kolmogorov-Smirnov test. Output related to the dissolved DMeHg in the reservoir for the decadal averages and confidence intervals were then used in the bioaccumulation and mercury mass balance model (BioHg) to determine possible changes in Hg bioaccumulation in Sacramento Blackfish.

### **Principal Findings and Significance**

- High flow events in the beginning of the century may contribute large amounts of Hg to enter the river system (as expressed at Fort Churchill) but these high flow events cause the channel to widen over time to cause the magnitude of flow depth and associated bank erosion to decrease over time. This, along with reduced spring and summer stream flows, can lead to significant decreases in THg and TMeHg loading in the spring and summer.
- Fort Churchill DHg concentrations increase noticeably during the summer/fall low-flow periods due to larger stream bottom area from channel widening and associated diffusion. However, the decrease in flow, however, causes DHg loads to decrease significantly during these seasons. In contrast, DHg loading increases significantly during the winter and spring months.
- The highest DMeHg concentrations at Fort Churchill occur during the lowest flows while the lowest concentrations occur during the highest flows. Subsequently, DMeHg loads decrease across all seasons, with largest and most significant decreases occurring in the spring and summer.

- The three sections of the reservoir differ in the response of their DMeHg concentrations, with a modest increase during the summer and fall in the South and Middle Basin and an overall decrease in the North Basin. This is due to the North Basin receiving inflow from the Truckee Canal, effectively diluting the concentrations of DMeHg. As flows decrease throughout the century, this inflow has a stronger dilution effect on the North Basin.
- Overall, the results from each of the three scenarios show the fish exceeding the federal consumption advisory level of 1 µg of Hg per g of mass by the end of their first year of life, and this is true for both the first and last decade of the century. These results suggest that the Sacramento blackfish will continue to be unsafe to consume throughout the century unless some sort of mitigation strategy is attempted

### **Information Transfer Activities**

Research results were presented one regional and one international conference.

- Flickinger, A. K., Carroll, R. W., Warwick, J. J., Schumer, R. (2015). Impact of Climate Change on Mercury Transport along the Carson River-Lahontan Reservoir System, Nevada Water Resources Association: Reno, NV, January 26, 2015-April 29, 2015
- Flickinger, A. K., Carroll, R. W., Warwick, J. J., Schumer, R. (2014). Impact of climate change on mercury transport along the Carson River-Lahontan Reservoir system, American Geophysical Union: San Francisco, CO, December 15, 2014-December 19, 2014, H31H-0734.

A Master thesis has been submitted to the University of Nevada, Reno and is currently being converted into a paper for peer review. Likely submittal to Journal of Ecologic Modeling.

In addition the following paper has been submitted for review.

- Carroll, R. W., Warwick, J. J. (2015). Modeling the Highly Dynamic Loading of Mercury Species in the Carson River and Lahontan Reservoir System, Nevada, *Science of the Total Environment*, Submitted

### **Student Support**

Allison Flickenger is supported at the Masters level within the Graduate Program of Hydrologic Sciences at the University of Nevada, Reno.

### References Cited

- Carroll, R.W.H. 2010. Modeling mercury transport and bioaccumulation in the Carson River and Lahontan Reservoir System, Nevada. Dissertation. University of Nevada, Reno. 170 pp.
- Intergovernmental Panel on Climate Change (IPCC). 2007. Climate Change 2007: The Physical Science Basis. Contribution of Working Group I to the Fourth Assessment Report of the Intergovernmental Panel on Climate Change. Solomon, S., D. Qin, M. Manning, Z. Chen, M. Marquis, K.B. Avery, M. Tignor, and H.L. Miller (eds.). Cambridge University Press, Cambridge, United Kingdom and New York, New York, United States, 996 pp. Available at <http://www.ipcc.ch/ipccreports/ar4-wg1.htm>.
- United States Bureau of Reclamation (USBR). 2011. West-wide climate risk assessments: bias-corrected and spatially downscaled surface water projections. Technical Memorandum no. 86-68210-2011-01. 138 pp.

United States. Global Change Research Program (USGCRP). 2009. Global Climate Change Impacts in the United States, T.R. Karl, J.M. Melillo, and T.C. Peterson, (eds.). Cambridge University Press, 196 pp.

# Information Transfer Program Introduction

None.

# USGS Summer Intern Program

None.

<b>Student Support</b>					
<b>Category</b>	<b>Section 104 Base Grant</b>	<b>Section 104 NCGP Award</b>	<b>NIWR-USGS Internship</b>	<b>Supplemental Awards</b>	<b>Total</b>
<b>Undergraduate</b>	1	0	0	0	1
<b>Masters</b>	4	0	0	0	4
<b>Ph.D.</b>	1	0	0	0	1
<b>Post-Doc.</b>	1	0	0	0	1
<b>Total</b>	7	0	0	0	7

## **Notable Awards and Achievements**

Dr. Gerrity leveraged the information gathered during this study (Optimization of Ozone-biological Activated Carbon Treatment for Potable Reuse Applications - 2013NV194B) and the existing pilot infrastructure to obtain additional external funding from the U.S. Environmental Protection Agency's STAR program: Early Career Awards Human and Ecological Health Impacts Associated with Water Reuse and Conservation Practices (EPA-G2014-STAR-F2). The three-year EPA project is expected to start in August 2015 and will support at least two graduate students and several undergraduate students.

## Publications from Prior Years

1. 2009NV150B ("Black Carbon in Sierra Nevada Snow: Impacts on Snowmelt and Water Supply") - Articles in Refereed Scientific Journals - Sterle, K.M., J.R. McConnell, J. Dozier, R. Edwards, and M. Flanner, Retention and radiative forcing of black carbon in eastern Sierra Nevada snow (2013) *The Cryosphere*, 7, 365-374, doi:10.5194/tc-7-365-2013.
2. 2011NV178B ("Measuring Water Use of Tamarisk and Impacts from Biocontrol: Lower Virgin River, NV") - Articles in Refereed Scientific Journals - Acharya, K., Sueki, S., Conrad, B., Dudley, T.L., Bean, D.W., and Osterberg, J.C. (2013) Life history characteristics of *Diorhabda carinulata* under Various Temperatures. *Environmental Entomology* 42: 546-571.
3. 2011NV178B ("Measuring Water Use of Tamarisk and Impacts from Biocontrol: Lower Virgin River, NV") - Articles in Refereed Scientific Journals - Conrad, B., Acharya, K., Dudley, T., and Bean, D. (2013) Episodic herbivory by the tamarisk beetle in *Tamarix ramosissima* increases leaf litter nitrogen and stem starch content: a short communication. *Journal of Arid Environments* 94: 76-79.
4. 2011NV178B ("Measuring Water Use of Tamarisk and Impacts from Biocontrol: Lower Virgin River, NV") - Conference Proceedings - Sueki, S., Acharya, K., Healey, J., Jasoni, R. (2013) Defoliation effect of leaf beetles on evapotranspiration from *Tamrix*. 2013 UCOWR/NIWR annual conference, Lake Tahoe, CA
5. 2011NV178B ("Measuring Water Use of Tamarisk and Impacts from Biocontrol: Lower Virgin River, NV") - Conference Proceedings - Acharya, K.; Sueki, S. (2011) Effect of temperature on *Diorhabda elongate* growth and mortality. Tamarisk Research Conference, Tamarisk Coalition, Tucson, AZ
6. 2011NV180B ("Effects of Regional Climate Change on Snowpack in Northern Nevada: Research and Education") - Articles in Refereed Scientific Journals - Backes, T. M., Kaplan, M. L., Schumer, R., Mejia, J. F. (2015). A Climatology of the Vertical Structure of Water Vapor Transport to the Sierra Nevada in Cool Season Atmospheric River Precipitation Events, *J. Hydrometeor.*, 16, (3), 1029-1047, doi: 10.1175/JHM-D-14-0077.1
7. 2011NV181B ("Quantifying the Impact of Hyporheic Exchange on In-Stream Water Quality in the Truckee River, NV") - Articles in Refereed Scientific Journals - Johnson, Z. C., Schumer, R., Warwick, J. J. (2014). Factors affecting hyporheic and surface transient storage in a western U.S. river, *Journal of Hydrology*, 510, 325--339, doi: 10.1016/j.jhydrol.2013.12.037
8. 2011NV181B ("Quantifying the Impact of Hyporheic Exchange on In-Stream Water Quality in the Truckee River, NV") - Articles in Refereed Scientific Journals - Johnson, Z. C., Warwick, J. J., Schumer, R. (2014). Nitrogen retention in the main channel and two transient storage zones during nutrient addition experiments, *Limnology and Oceanography*, DOI:10.1002/lno.10006, doi: 10.1002/lno.10006